



21st June 2023

Beta decay studies in the HISPEC/DESPEC FAIR Phase-0 campaign at GSI

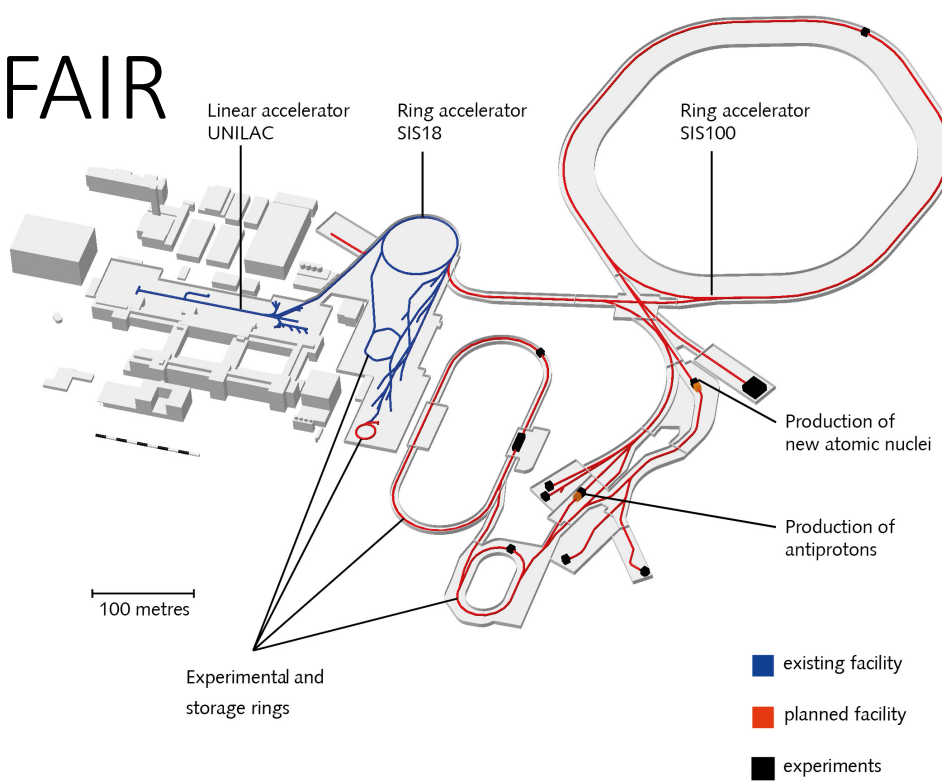
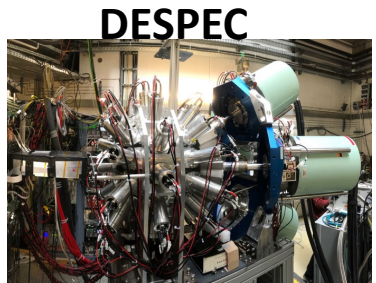
Marta Polettini

University and INFN Padova



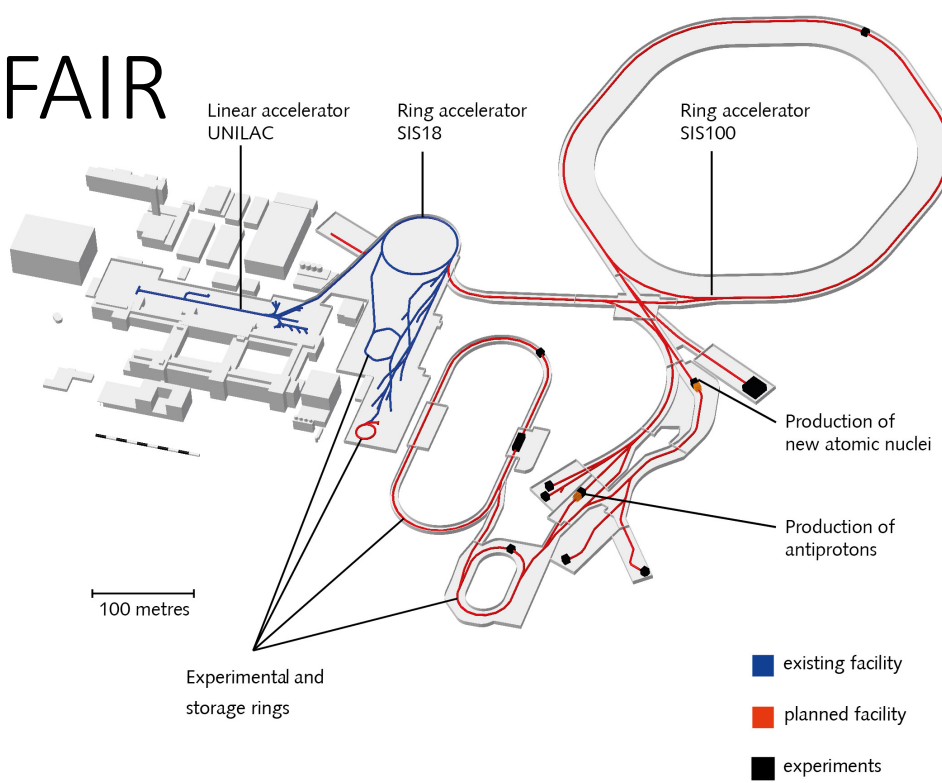
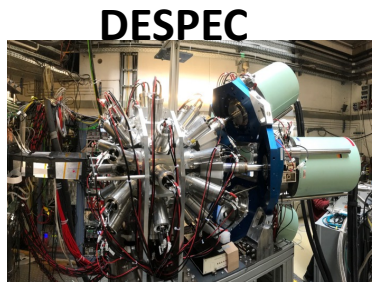
HISPEC-DESPEC at GSI-FAIR

Spectroscopic studies both **in-beam** (HISPEC) and with **stopped ions** (DESPEC).



HISPEC-DESPEC at GSI-FAIR

Spectroscopic studies both **in-beam** (HISPEC) and with **stopped ions** (DESPEC).



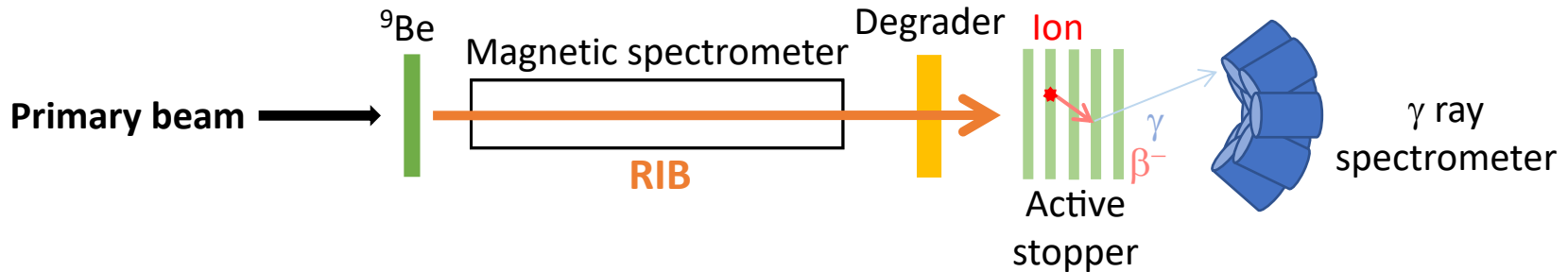
Strength of HISPEC/DESPEC:

Use combination of unique detectors for complete spectroscopy of exotic nuclei with yields as low as **one ion per hour** (~nb)

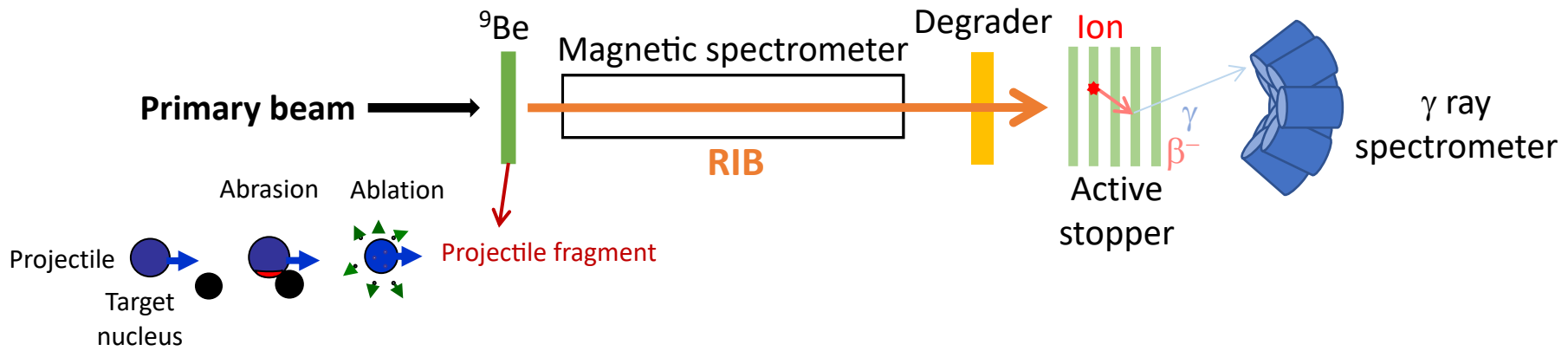
Key goals exploiting unique GSI-FAIR beams:

- Approach the r-process path along N=126: **nucleosynthesis of heavy nuclei**
- Evolution of the shell structure and exotic nuclear shapes in **uncharted nuclear territory**

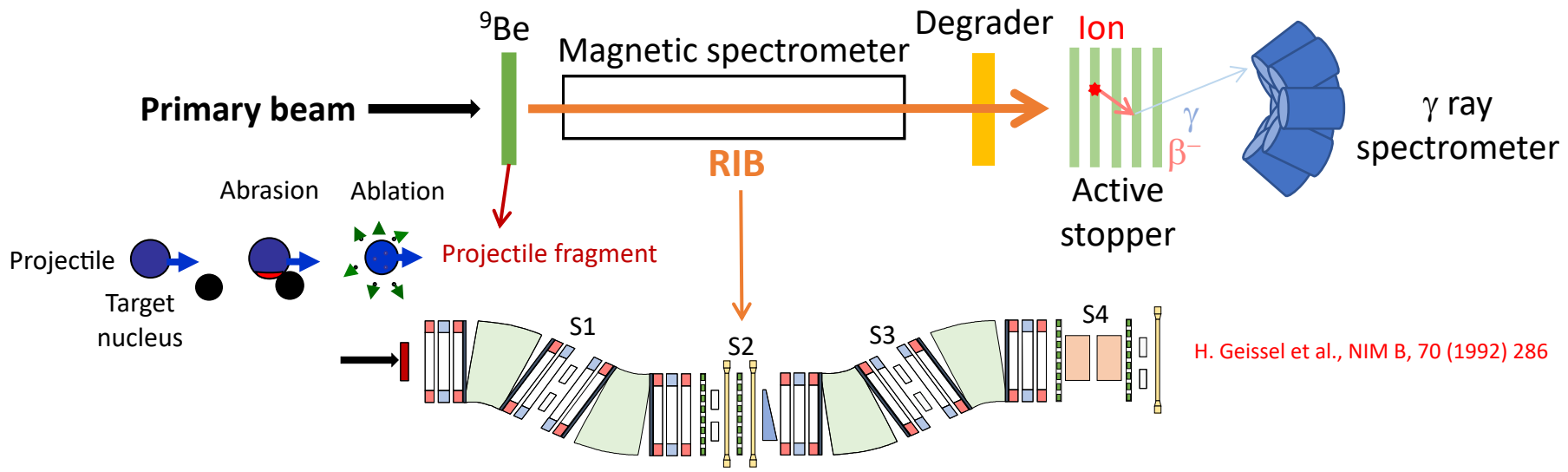
The FRS+DESPEC setup



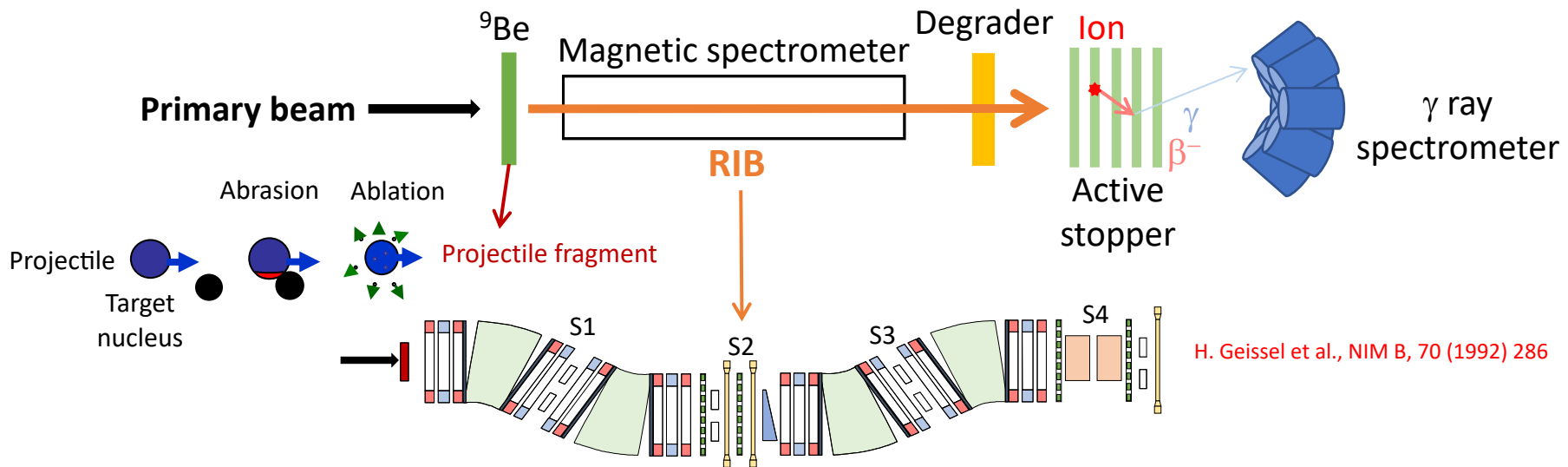
The FRS+DESPEC setup



The FRS+DESPEC setup



The FRS+DESPEC setup

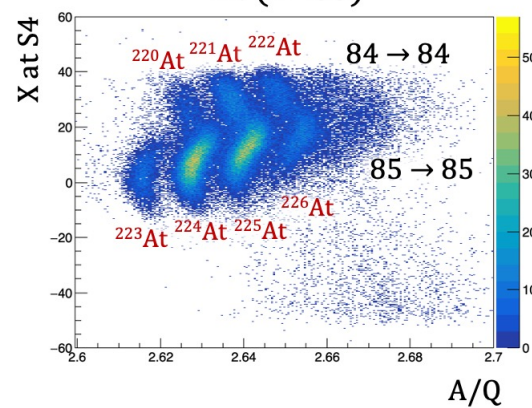
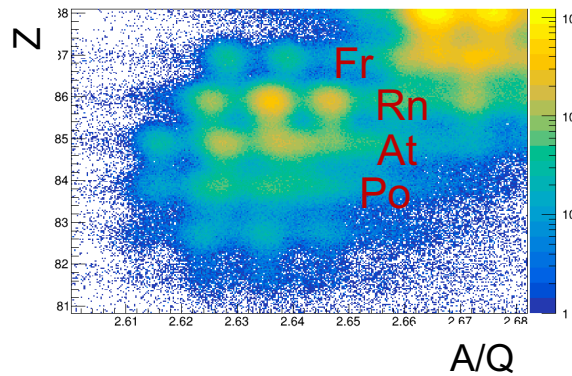


Selection and identification:

$$B\rho - \Delta E - B\rho$$

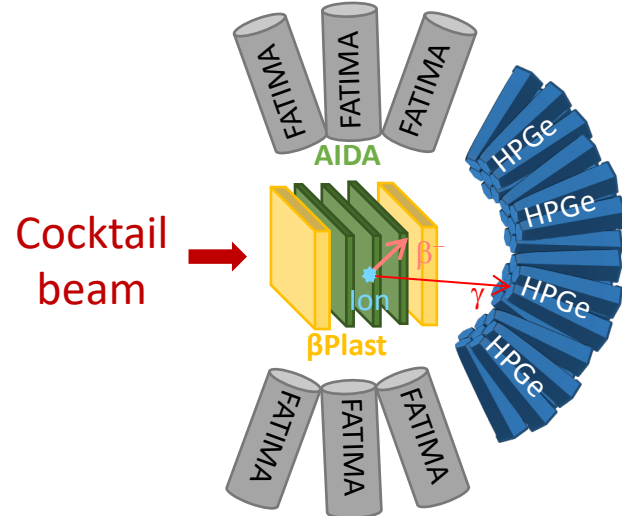
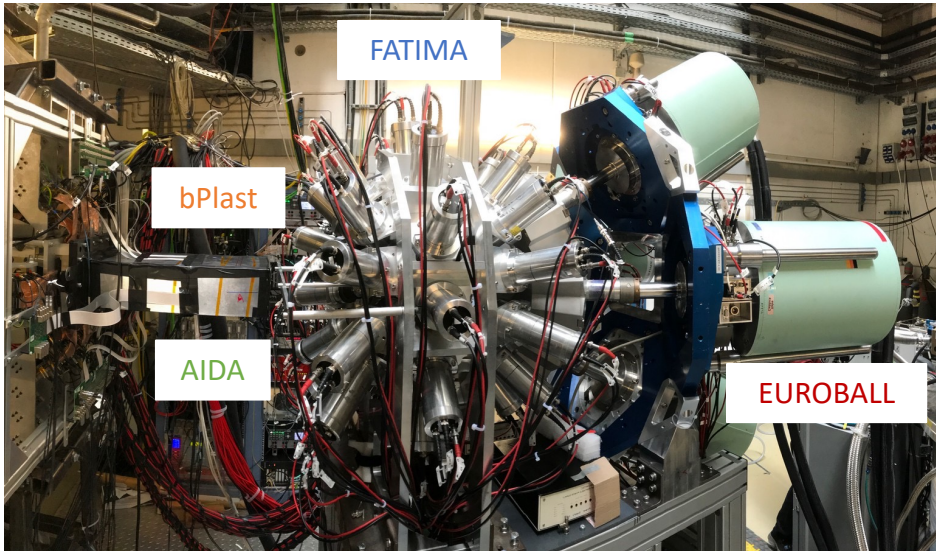
&

$$ToF - B\rho - \Delta E$$



The DESPEC station

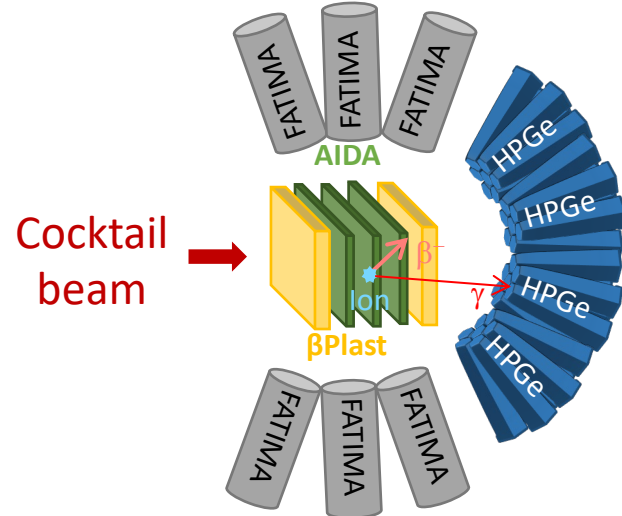
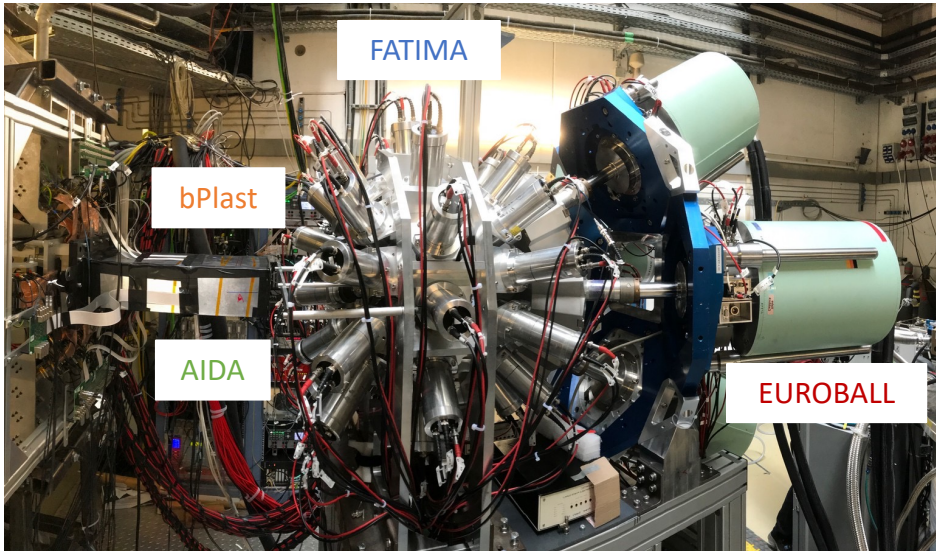
A. K. Mistry et al., NIM A 1033 (2022) 166662



- **AIDA:** 8x8 cm² DSSSD tiles, 16384 pixels
- **bPlast:** BC-400 plastic detector
- **Euroball:** four 7-fold HPGe clusters
- **FATIMA:** 36 LaBr₃(Ce) detectors

The DESPEC station

A. K. Mistry et al., NIM A 1033 (2022) 166662

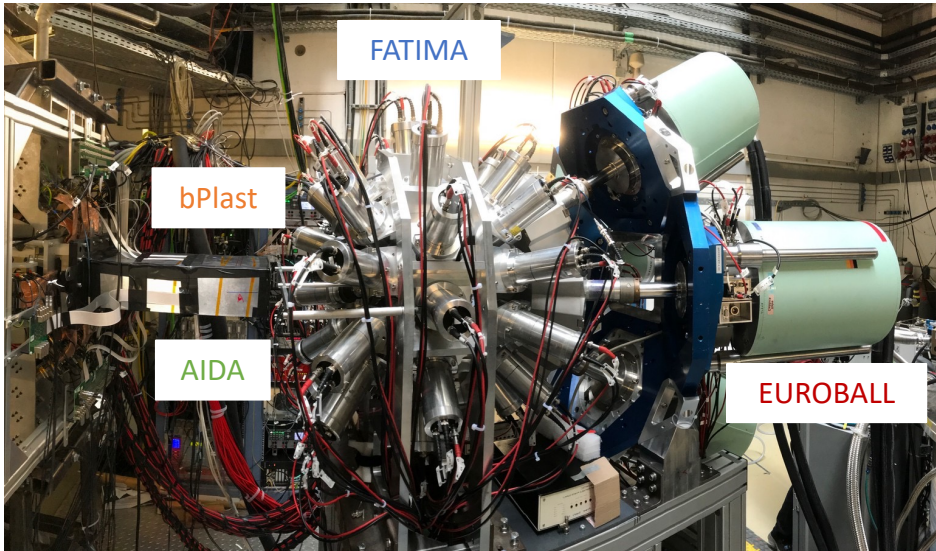


- **AIDA:** 8x8 cm² DSSSD tiles, 16384 pixels
- **bPlast:** BC-400 plastic detector
- **Euroball:** four 7-fold HPGe clusters
- **FATIMA:** 36 LaBr₃(Ce) detectors

Ion → β decay → γ rays

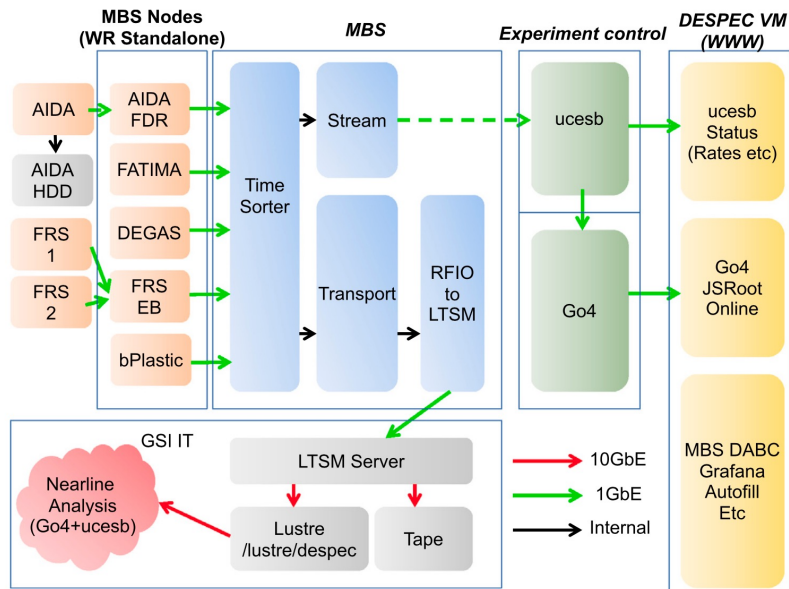
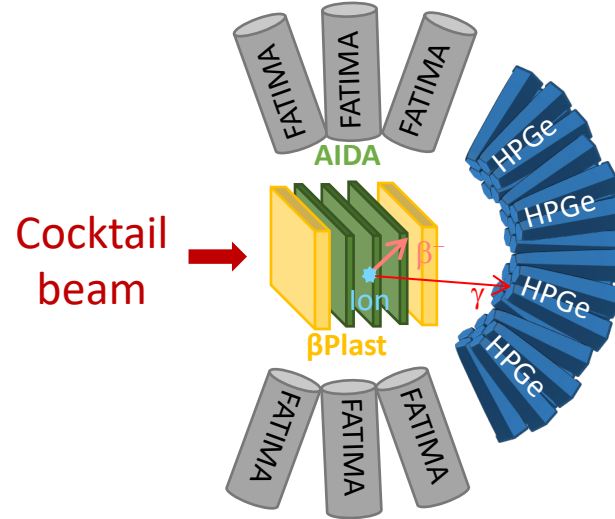
The DESPEC station

A. K. Mistry et al., NIM A 1033 (2022) 166662



- **AIDA:** 8x8 cm² DSSSD tiles, 16384 pixels
- **bPlast:** BC-400 plastic detector
- **Euroball:** four 7-fold HPGe clusters
- **FATIMA:** 36 LaBr₃(Ce) detectors

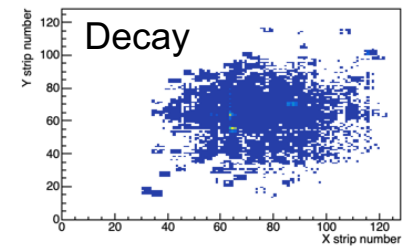
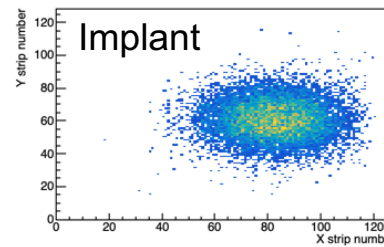
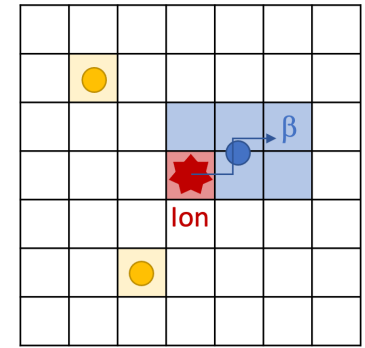
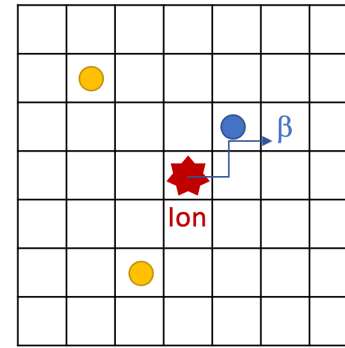
Ion → β decay → γ rays



Ion– β – γ correlations

Ion– β correlations:

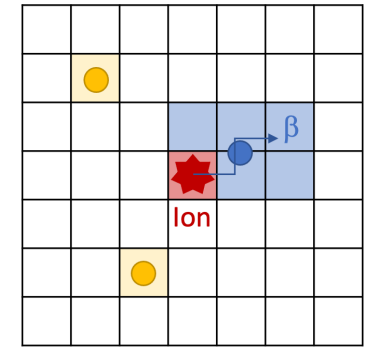
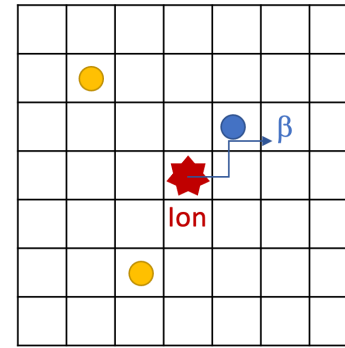
- Position condition \rightarrow ion and β cluster overlap
- Time condition \rightarrow $dT(Ion - \beta) < 5\tau_\beta$



Ion- β - γ correlations

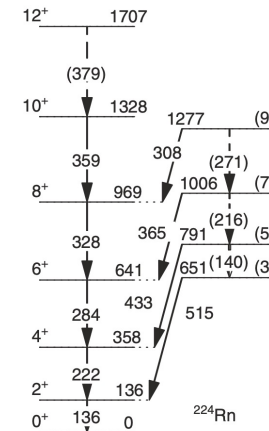
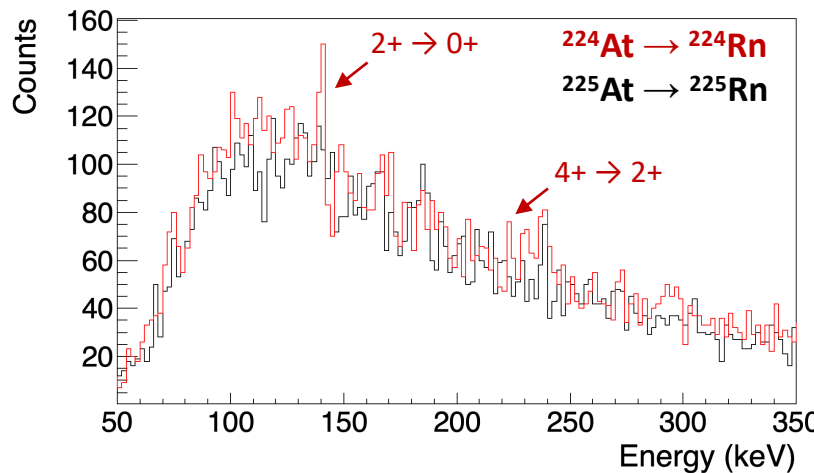
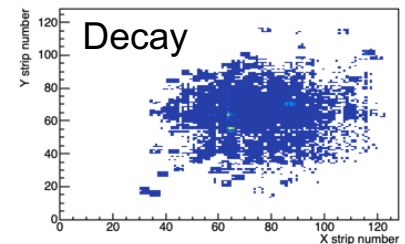
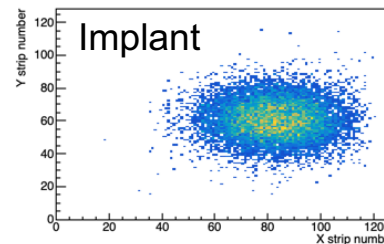
Ion- β correlations:

- Position condition \rightarrow ion and β cluster overlap
- Time condition \rightarrow $dT(Ion - \beta) < 5\tau_\beta$



β - γ correlations:

- Prompt coincidence: $\Delta T(\gamma - \beta) < 100\text{ ns}$



P. A. Butler et al., Nat. Commun. 10 (2019) 2473

INFN experiments in FAIR Phase-0 campaign

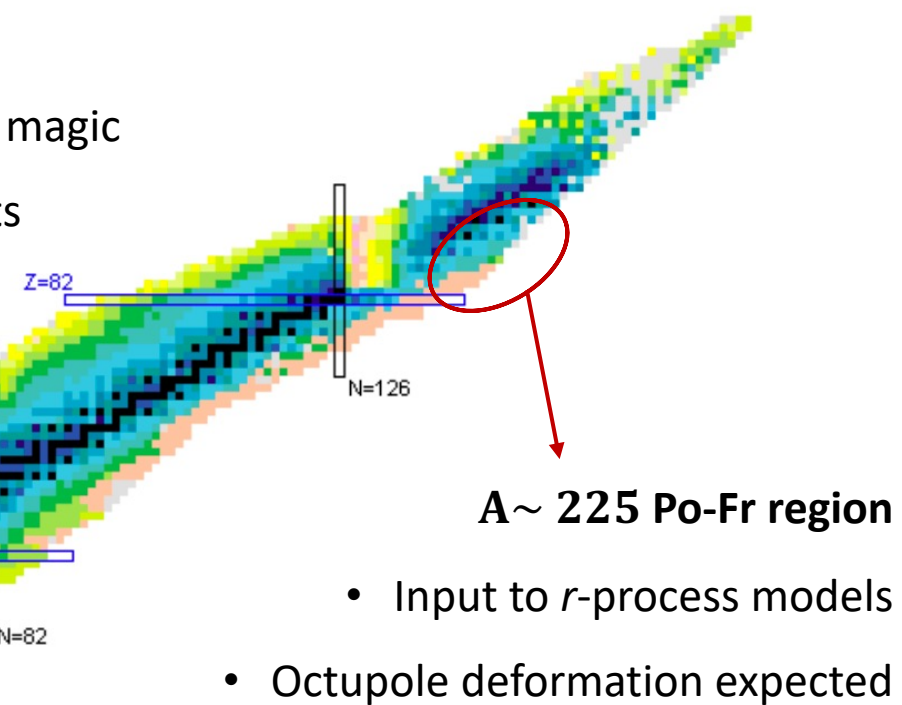
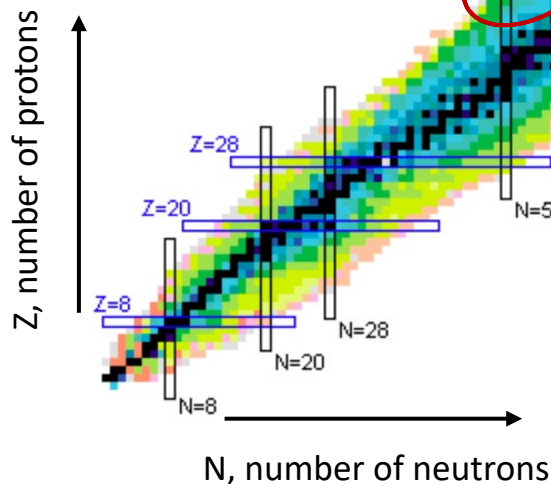
^{124}Xe beam

840 MeV/u

		Xenon Z=54	^{108}Xe	^{109}Xe	^{110}Xe	^{111}Xe
	Iodine Z=53	^{106}I	^{107}I	^{108}I	^{109}I	^{110}I
	Tellurium Z=52	^{104}Te	^{105}Te	^{106}Te	^{107}Te	^{108}Te
	Antimony Z=51	^{102}Sb	^{103}Sb	^{104}Sb	^{105}Sb	^{106}Sb
	Tin Z=50	^{99}Sn	^{100}Sn	^{101}Sn	^{102}Sn	^{103}Sn
Indium Z=49		^{97}In	^{98}In	^{99}In	^{100}In	^{101}In
Cadmium Z=48		^{96}Cd	^{97}Cd	^{98}Cd	^{99}Cd	^{100}Cd
Silver Z=47		^{95}Ag	^{96}Ag	^{97}Ag	^{98}Ag	^{99}Ag
Palladium Z=46		^{94}Pd	^{95}Pd	^{96}Pd	^{97}Pd	^{98}Pd
Rhodium Z=45		^{93}Rh	^{94}Rh	^{95}Rh	^{96}Rh	^{97}Rh
Ruthenium Z=44		^{92}Ru	^{93}Ru	^{94}Ru	^{95}Ru	^{96}Ru
		^{97}Ru	^{98}Ru	^{99}Ru	^{100}Ru	^{101}Ru

^{100}Sn region

- $N = Z = 50$ doubly magic
- Core-breaking effects



Radium Z=88	^{217}Ra	^{218}Ra	^{219}Ra	^{220}Ra	^{221}Ra	^{222}Ra	^{223}Ra	^{224}Ra	^{225}Ra	^{226}Ra	^{227}Ra	^{228}Ra	^{229}Ra	^{230}Ra	^{231}Ra	^{232}Ra	^{233}Ra	^{234}Ra	^{235}Ra
Francium Z=87	^{216}Fr	^{217}Fr	^{218}Fr	^{219}Fr	^{220}Fr	^{221}Fr	^{222}Fr	^{223}Fr	^{224}Fr	^{225}Fr	^{226}Fr	^{227}Fr	^{228}Fr	^{229}Fr	^{230}Fr	^{231}Fr	^{232}Fr	^{233}Fr	
Radon Z=86	^{215}Rn	^{216}Rn	^{217}Rn	^{218}Rn	^{219}Rn	^{220}Rn	^{221}Rn	^{222}Rn	^{223}Rn	^{224}Rn	^{225}Rn	^{226}Rn	^{227}Rn	^{228}Rn	^{229}Rn	^{230}Rn	^{231}Rn		
Astatine Z=85	^{214}At	^{215}At	^{216}At	^{217}At	^{218}At	^{219}At	^{220}At	^{221}At	^{222}At	^{223}At	^{224}At	^{225}At	^{226}At	^{227}At	^{228}At	^{229}At			
Polonium Z=84	^{213}Po	^{214}Po	^{215}Po	^{216}Po	^{217}Po	^{218}Po	^{219}Po	^{220}Po	^{221}Po	^{222}Po	^{223}Po	^{224}Po	^{225}Po	^{226}Po	^{227}Po				
Bismuth Z=83	^{212}Bi	^{213}Bi	^{214}Bi	^{215}Bi	^{216}Bi	^{217}Bi	^{218}Bi	^{219}Bi	^{220}Bi	^{221}Bi	^{222}Bi	^{223}Bi	^{224}Bi						
Lead Z=82	^{211}Pb	^{212}Pb	^{213}Pb	^{214}Pb	^{215}Pb	^{216}Pb	^{217}Pb	^{218}Pb	^{219}Pb	^{220}Pb									
Thallium Z=81	^{210}Tl	^{211}Tl	^{212}Tl	^{213}Tl	^{214}Tl	^{215}Tl	^{216}Tl	^{217}Tl	^{218}Tl										

^{238}U beam
1 GeV/u

INFN experiments in FAIR Phase-0 campaign

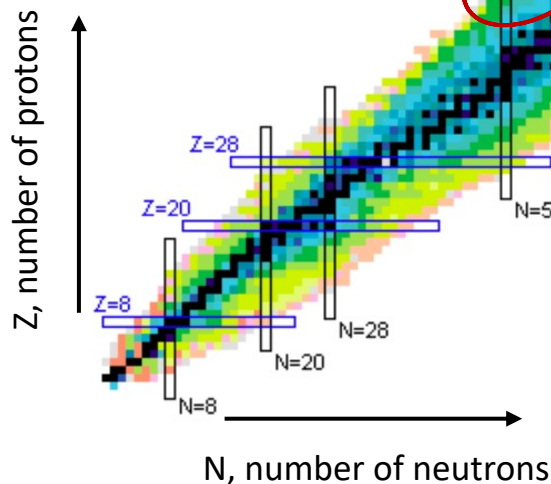
^{124}Xe beam

840 MeV/u

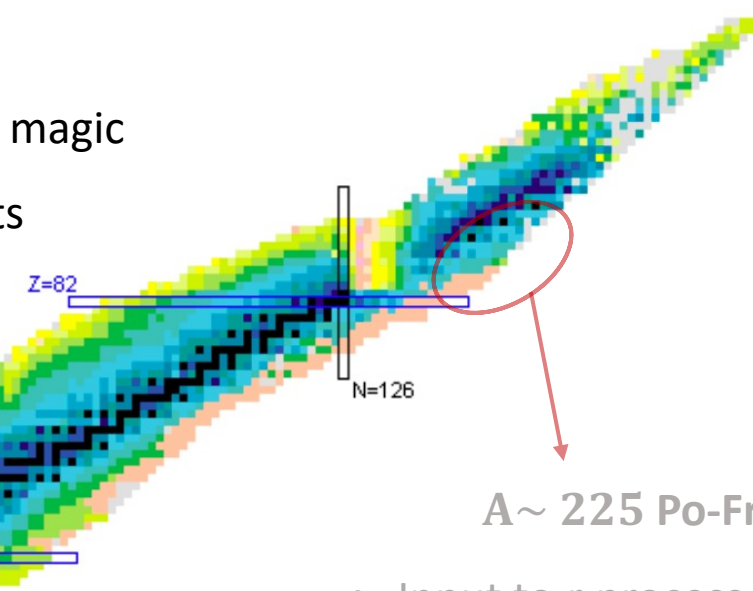
		Xenon Z=54	^{108}Xe	^{109}Xe	^{110}Xe	^{111}Xe
	Iodine Z=53	^{106}I	^{107}I	^{108}I	^{109}I	^{110}I
	Tellurium Z=52	^{104}Te	^{105}Te	^{106}Te	^{107}Te	^{108}Te
	Antimony Z=51	^{102}Sb	^{103}Sb	^{104}Sb	^{105}Sb	^{106}Sb
	Tin Z=50	^{99}Sn	^{100}Sn	^{101}Sn	^{102}Sn	^{103}Sn
Indium Z=49	^{97}In	^{98}In	^{99}In	^{100}In	^{101}In	^{102}In
Cadmium Z=48	^{96}Cd	^{97}Cd	^{98}Cd	^{99}Cd	^{100}Cd	^{101}Cd
Silver Z=47	^{95}Ag	^{96}Ag	^{97}Ag	^{98}Ag	^{99}Ag	^{100}Ag
Palladium Z=46	^{94}Pd	^{95}Pd	^{96}Pd	^{97}Pd	^{98}Pd	^{99}Pd
Rhodium Z=45	^{93}Rh	^{94}Rh	^{95}Rh	^{96}Rh	^{97}Rh	^{98}Rh
Ruthenium Z=44	^{92}Ru	^{93}Ru	^{94}Ru	^{95}Ru	^{96}Ru	^{97}Ru
		^{98}Ru	^{99}Ru	^{100}Ru	^{101}Ru	

^{100}Sn region

- $N = Z = 50$ doubly magic
- Core-breaking effects



Marta Polettini



- Input to r -process models
- Octupole deformation expected

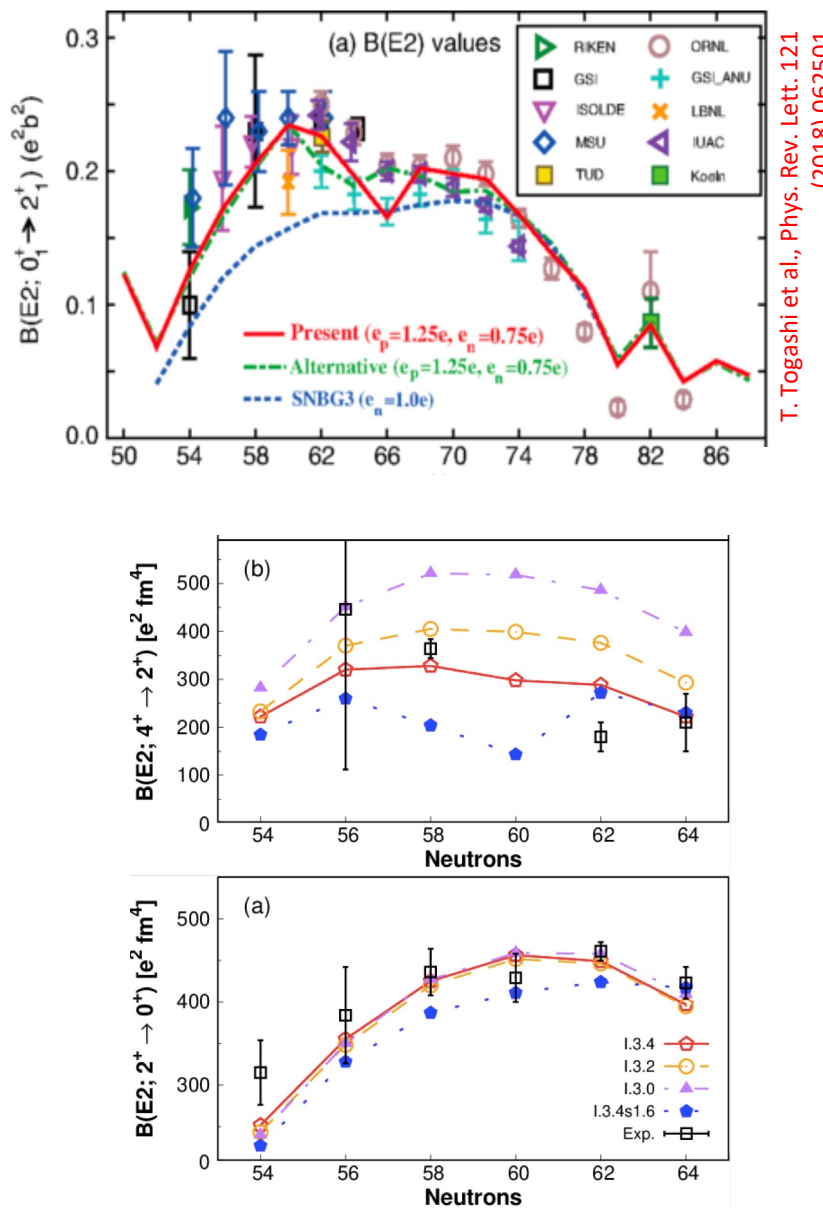
Radium Z=88	^{217}Ra	^{218}Ra	^{219}Ra	^{220}Ra	^{221}Ra	^{222}Ra	^{223}Ra	^{224}Ra	^{225}Ra	^{226}Ra	^{227}Ra	^{228}Ra	^{229}Ra	^{230}Ra	^{231}Ra	^{232}Ra	^{233}Ra	^{234}Ra	^{235}Ra
Francium Z=87	^{216}Fr	^{217}Fr	^{218}Fr	^{219}Fr	^{220}Fr	^{221}Fr	^{222}Fr	^{223}Fr	^{224}Fr	^{225}Fr	^{226}Fr	^{227}Fr	^{228}Fr	^{229}Fr	^{230}Fr	^{231}Fr	^{232}Fr	^{233}Fr	
Radon Z=86	^{215}Rn	^{216}Rn	^{217}Rn	^{218}Rn	^{219}Rn	^{220}Rn	^{221}Rn	^{222}Rn	^{223}Rn	^{224}Rn	^{225}Rn	^{226}Rn	^{227}Rn	^{228}Rn	^{229}Rn	^{230}Rn	^{231}Rn		
Astatine Z=85	^{214}At	^{215}At	^{216}At	^{217}At	^{218}At	^{219}At	^{220}At	^{221}At	^{222}At	^{223}At	^{224}At	^{225}At	^{226}At	^{227}At	^{228}At	^{229}At			
Polonium Z=84	^{213}Po	^{214}Po	^{215}Po	^{216}Po	^{217}Po	^{218}Po	^{219}Po	^{220}Po	^{221}Po	^{222}Po	^{223}Po	^{224}Po	^{225}Po	^{226}Po	^{227}Po				
Bismuth Z=83	^{212}Bi	^{213}Bi	^{214}Bi	^{215}Bi	^{216}Bi	^{217}Bi	^{218}Bi	^{219}Bi	^{220}Bi	^{221}Bi	^{222}Bi	^{223}Bi	^{224}Bi						
Lead Z=82	^{211}Pb	^{212}Pb	^{213}Pb	^{214}Pb	^{215}Pb	^{216}Pb	^{217}Pb	^{218}Pb	^{219}Pb	^{220}Pb									
Thallium Z=81	^{210}Tl	^{211}Tl	^{212}Tl	^{213}Tl	^{214}Tl	^{215}Tl	^{216}Tl	^{217}Tl	^{218}Tl										

^{238}U beam
1 GeV/u

The ^{100}Sn region

The ^{100}Sn region is subject of a multitude of experimental and theoretical studies to assess:

- the robustness of its **double shell closure**
- the evolution of **single-particle energies**
- the role of **proton-neutron pairing**



A. P. Zuker et al., Phys. Rev. C 103, 024322 (2021)
M. Siciliano et al., Phys. Lett. B 806, 135474 (2020)

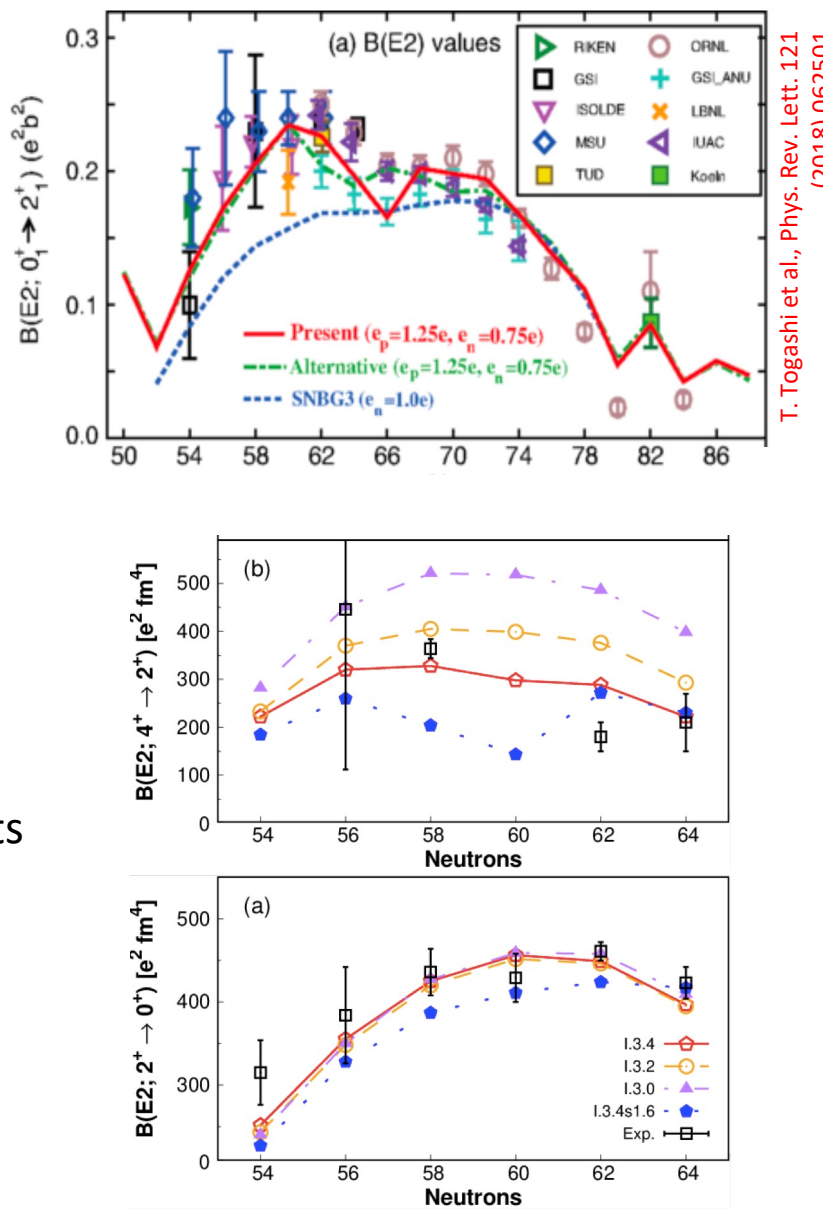
The ^{100}Sn region

The ^{100}Sn region is subject of a multitude of experimental and theoretical studies to assess:

- the robustness of its **double shell closure**
- the evolution of **single-particle energies**
- the role of **proton-neutron pairing**

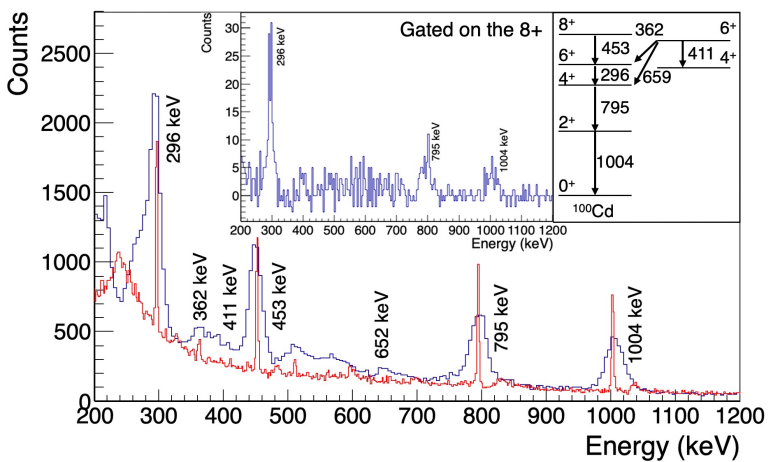
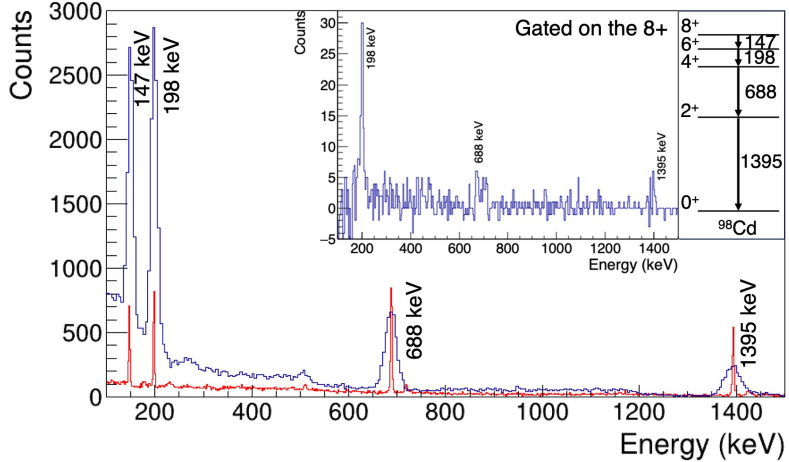
^{48}Cd isotopic chain \rightarrow two proton holes in $g_{9/2}$ orbits

- B(E2) measurements of levels below seniority isomers
- Beta decay spectroscopy studies

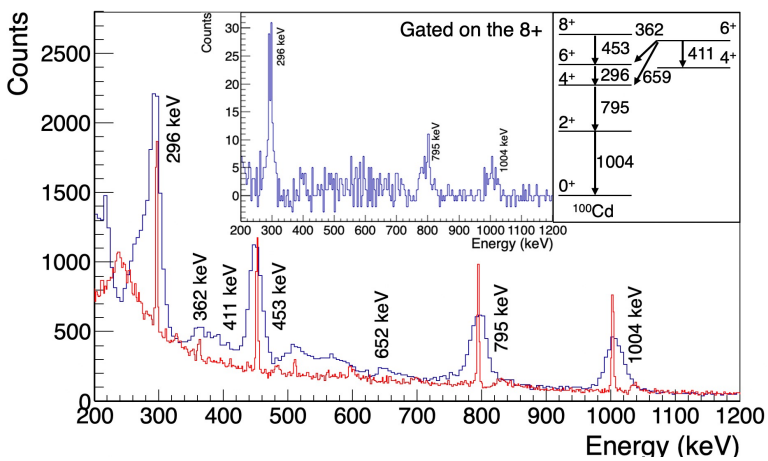
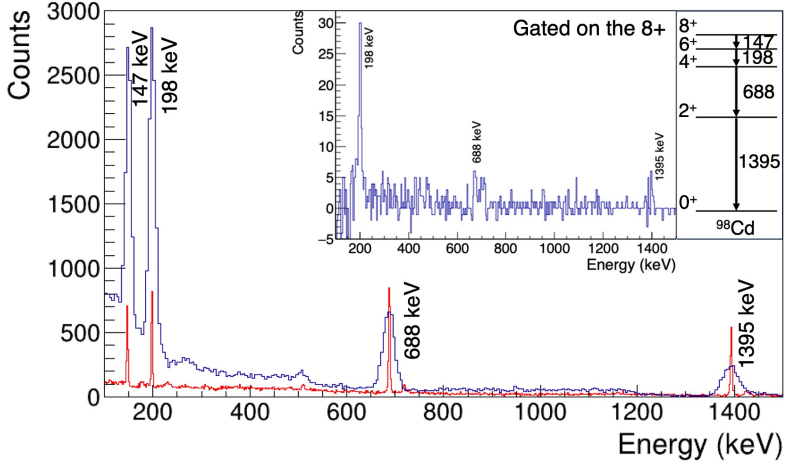


A. P. Zuker et al., Phys. Rev. C 103, 024322 (2021)
M. Siciliano et al., Phys. Lett. B 806, 135474 (2020)

$^{98,100}\text{Cd}$ levels' lifetimes



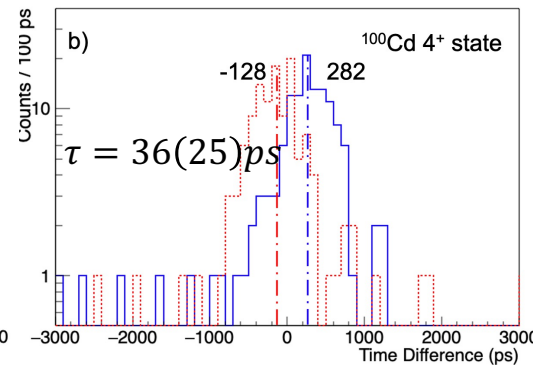
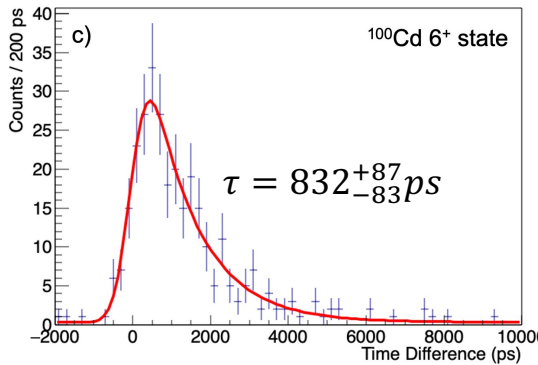
$^{98,100}\text{Cd}$ levels' lifetimes



- The **lifetimes of low-lying excited states below the 8^+** seniority isomer were directly measured in $^{98,100}\text{Cd}$
- B(E2) values** extracted using measured levels' lifetimes
- Comparison with shell model calculations** being investigated

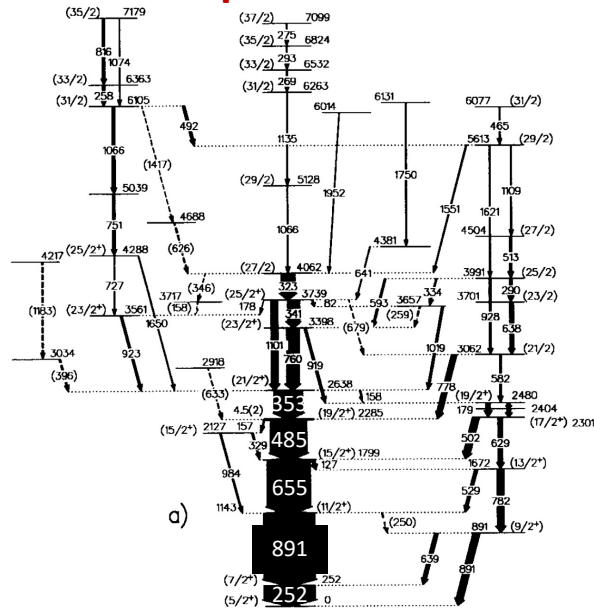
Calculations performed by:

A. Gargano, G. De Gregorio - INFN Napoli
F. Nowacki - Uni Strasbourg



^{101}Cd : first measurement of I_β and $\log ft$

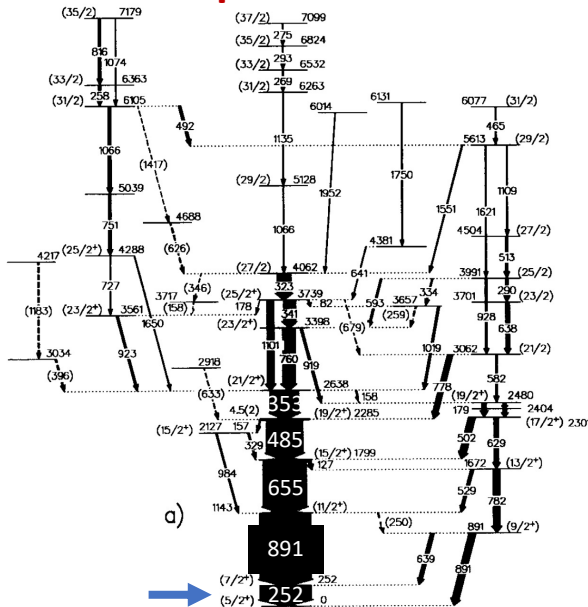
Fusion-evaporation reaction



M. Palacz et al., Nucl. Phys. A 608 (1996) 227–242

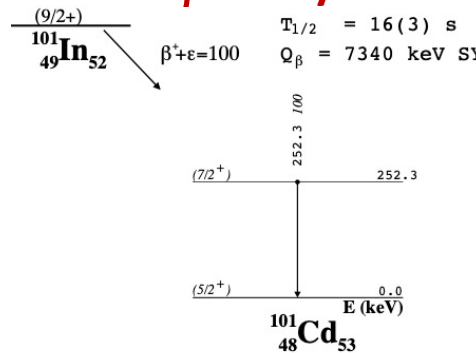
^{101}Cd : first measurement of I_β and $\log ft$

Fusion-evaporation reaction



M. Palacz et al., Nucl. Phys. A 608 (1996) 227–242

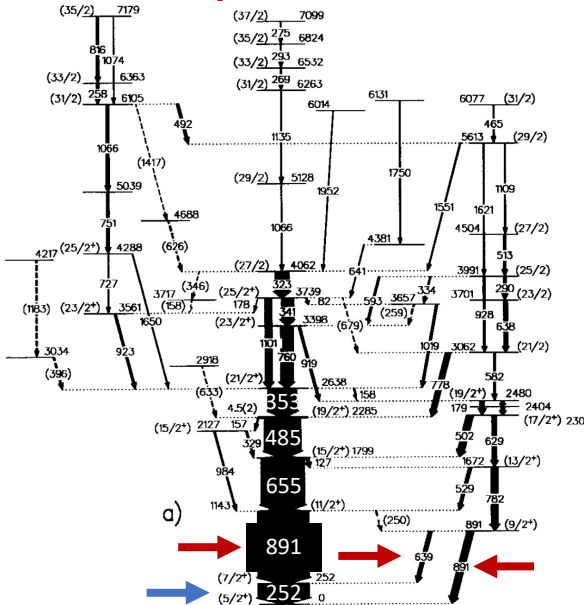
β decay



M. Huyse et al., Z. Phys. A 330 (1988) 121–122

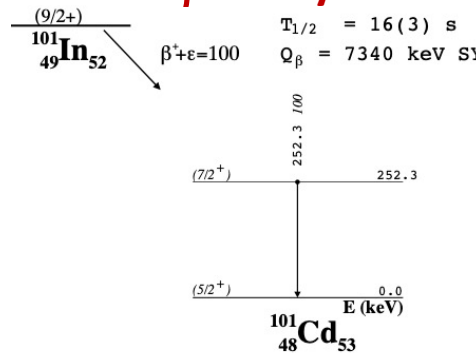
^{101}Cd : first measurement of I_β and $\log ft$

Fusion-evaporation reaction

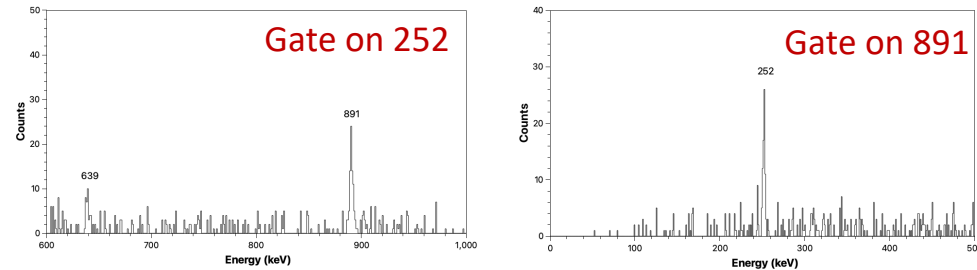


M. Palacz et al., Nucl. Phys. A 608 (1996) 227–242

β decay

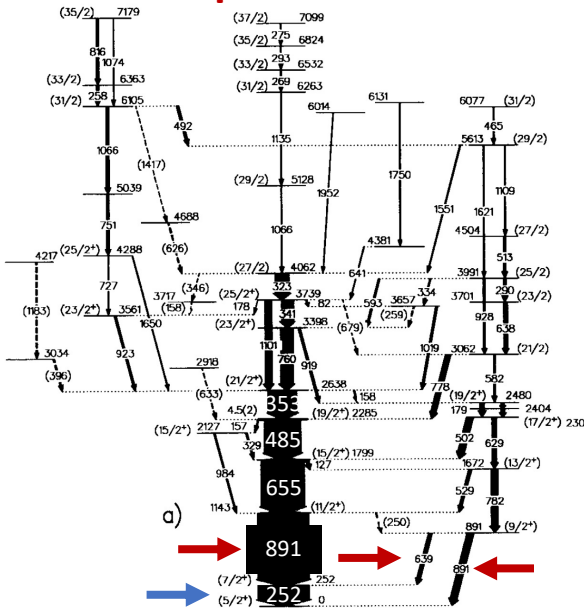


M. Huyse et al., Z. Phys. A 330 (1988) 121–122

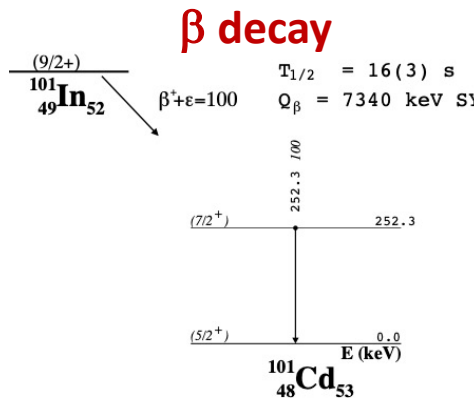


^{101}Cd : first measurement of I_β and $\log ft$

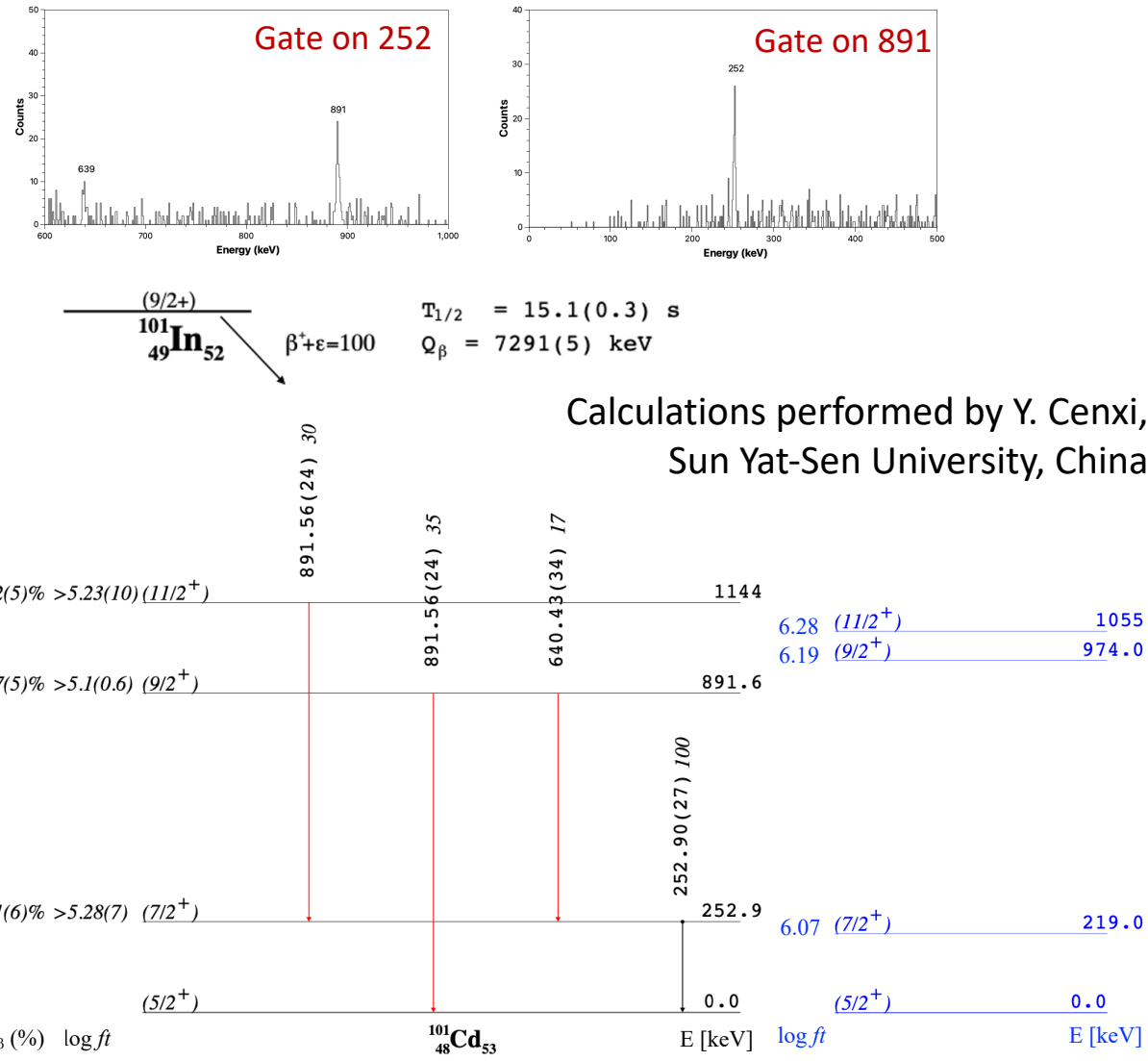
Fusion-evaporation reaction



M. Palacz et al., Nucl. Phys. A 608 (1996) 227–242



M. Huyse et al., Z. Phys. A 330 (1988) 121–122



INFN experiments in HISPEC-DESPEC in 2021

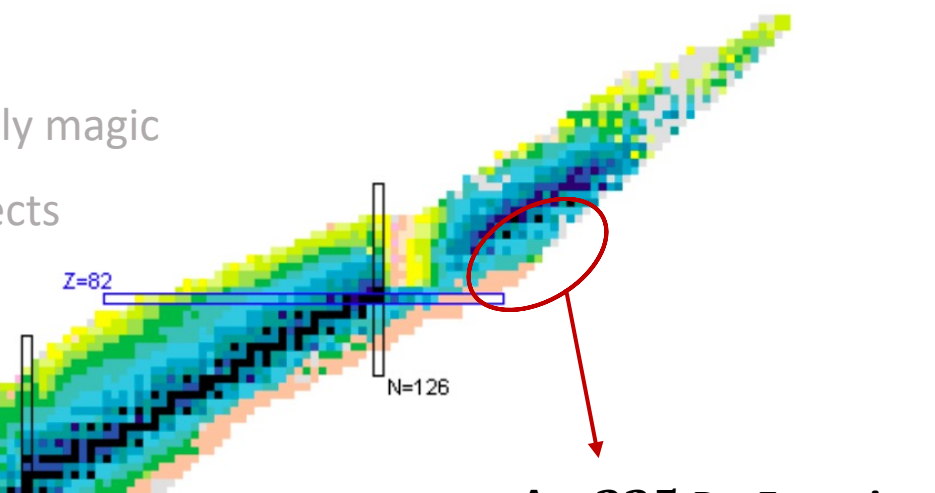
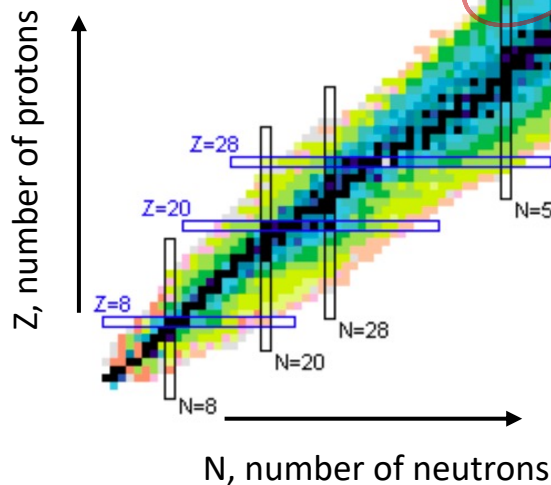
^{124}Xe beam

840 MeV/u

	Xenon Z=54	^{108}Xe	^{109}Xe	^{110}Xe	^{111}Xe
	Iodine Z=53	^{106}I	^{107}I	^{108}I	^{109}I
	Tellurium Z=52	^{104}Te	^{105}Te	^{106}Te	^{107}Te
	Antimony Z=51	^{102}Sb	^{103}Sb	^{104}Sb	^{105}Sb
	Tin Z=50	^{99}Sn	^{100}Sn	^{101}Sn	^{102}Sn
Indium Z=49	^{97}In	^{98}In	^{99}In	^{100}In	^{101}In
Cadmium Z=48	^{96}Cd	^{97}Cd	^{98}Cd	^{99}Cd	^{100}Cd
Silver Z=47	^{95}Ag	^{96}Ag	^{97}Ag	^{98}Ag	^{99}Ag
Palladium Z=46	^{94}Pd	^{95}Pd	^{96}Pd	^{97}Pd	^{98}Pd
Rhodium Z=45	^{93}Rh	^{94}Rh	^{95}Rh	^{96}Rh	^{97}Rh
Ruthenium Z=44	^{92}Ru	^{93}Ru	^{94}Ru	^{95}Ru	^{96}Ru

100 Sn region

- $N = Z = 50$ doubly magic
- Core-breaking effects



A ~ 225 Po-Fr region

- Input to r -process models
- Octupole deformation expected

Radium Z=88	^{217}Ra	^{218}Ra	^{219}Ra	^{220}Ra	^{221}Ra	^{222}Ra	^{223}Ra	^{224}Ra	^{225}Ra	^{226}Ra	^{227}Ra	^{228}Ra	^{229}Ra	^{230}Ra	^{231}Ra	^{232}Ra	^{233}Ra	^{234}Ra	^{235}Ra
Francium Z=87	^{216}Fr	^{217}Fr	^{218}Fr	^{219}Fr	^{220}Fr	^{221}Fr	^{222}Fr	^{223}Fr	^{224}Fr	^{225}Fr	^{226}Fr	^{227}Fr	^{228}Fr	^{229}Fr	^{230}Fr	^{231}Fr	^{232}Fr	^{233}Fr	
Radon Z=86	^{215}Rn	^{216}Rn	^{217}Rn	^{218}Rn	^{219}Rn	^{220}Rn	^{221}Rn	^{222}Rn	^{223}Rn	^{224}Rn	^{225}Rn	^{226}Rn	^{227}Rn	^{228}Rn	^{229}Rn	^{230}Rn	^{231}Rn		
Astatine Z=85	^{214}At	^{215}At	^{216}At	^{217}At	^{218}At	^{219}At	^{220}At	^{221}At	^{222}At	^{223}At	^{224}At	^{225}At	^{226}At	^{227}At	^{228}At	^{229}At			
Polonium Z=84	^{213}Po	^{214}Po	^{215}Po	^{216}Po	^{217}Po	^{218}Po	^{219}Po	^{220}Po	^{221}Po	^{222}Po	^{223}Po	^{224}Po	^{225}Po	^{226}Po	^{227}Po				
Bismuth Z=83	^{212}Bi	^{213}Bi	^{214}Bi	^{215}Bi	^{216}Bi	^{217}Bi	^{218}Bi	^{219}Bi	^{220}Bi	^{221}Bi	^{222}Bi	^{223}Bi	^{224}Bi						
Lead Z=82	^{211}Pb	^{212}Pb	^{213}Pb	^{214}Pb	^{215}Pb	^{216}Pb	^{217}Pb	^{218}Pb	^{219}Pb	^{220}Pb									
Thallium Z=81	^{210}Tl	^{211}Tl	^{212}Tl	^{213}Tl	^{214}Tl	^{215}Tl	^{216}Tl	^{217}Tl	^{218}Tl										

238U beam
1 GeV/u

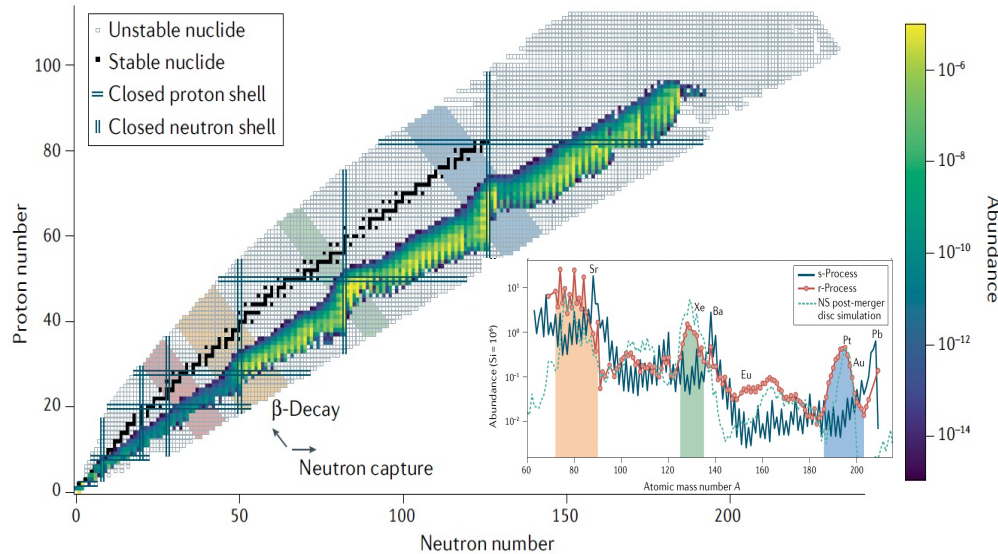
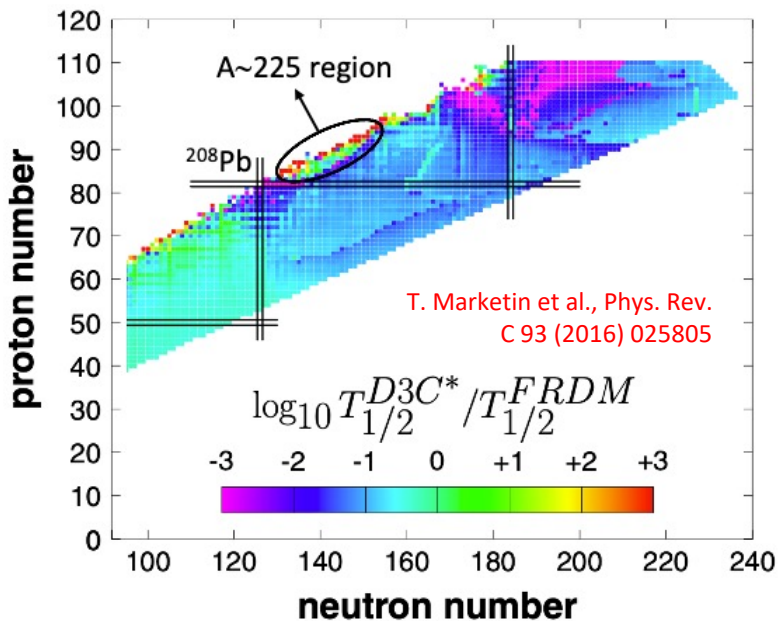
The A~225 region

Octupole deformation around A~225

- Locate low-lying 1^- and 3^- states
- Measure reduced transition strengths

Test of nuclear models for *r* process

- Measurement of ground state β -decay half-lives
- Determination of possible competing α branches

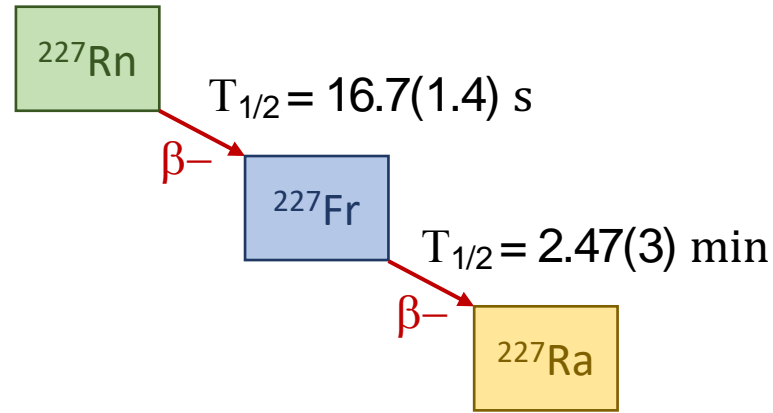
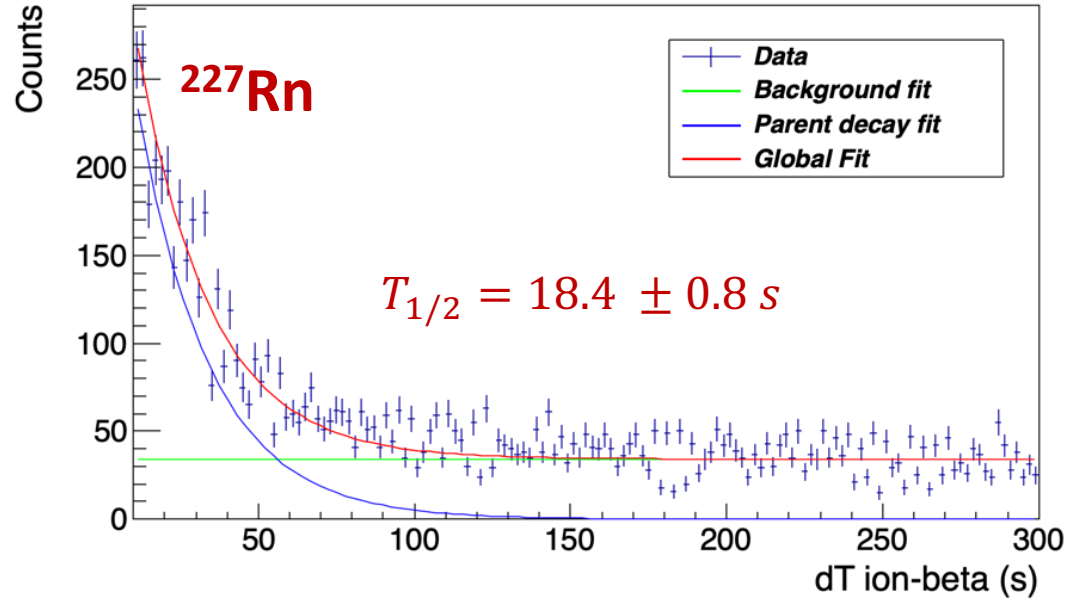


D. M. Siegel, Nat Rev Phys 4, 306–318 (2022)

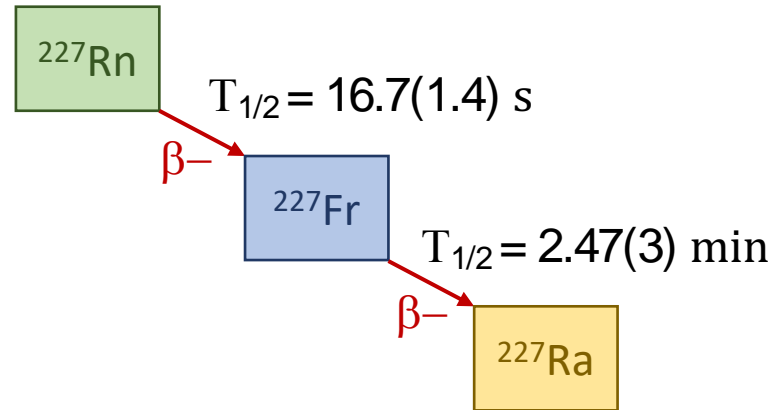
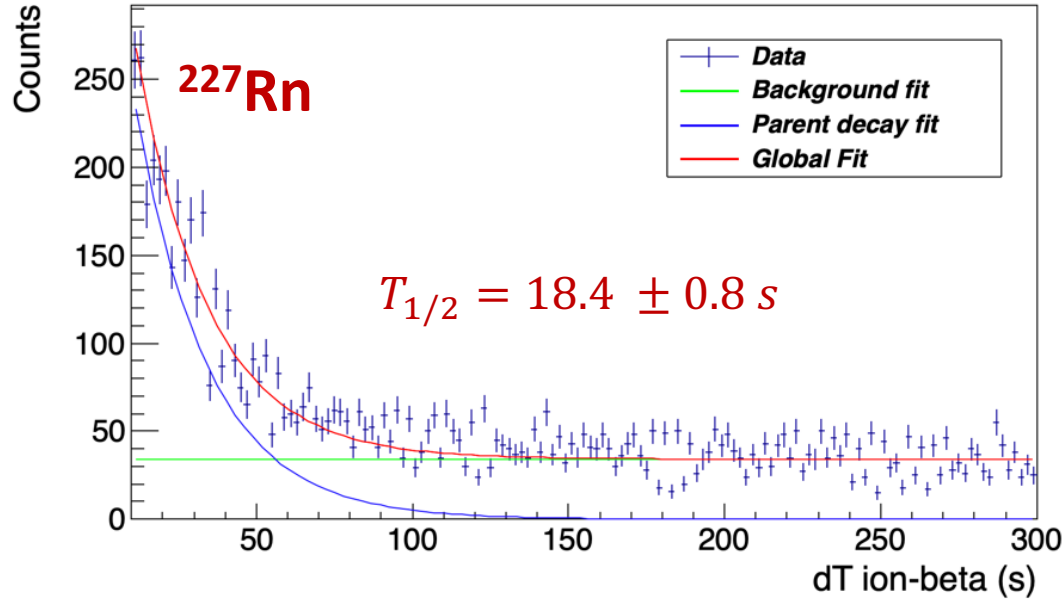
The *r* process:

- Neutron capture at a very short time scale as compared to β decay
- One of the main synthesis mode of elements up to $A \sim 200$
- Three abundance peaks at $A \sim 80, 130, 195$ ($N = 50, 82, 126$ shell closures)

New β -decay half-lives in At and Po isotopes



New β -decay half-lives in At and Po isotopes

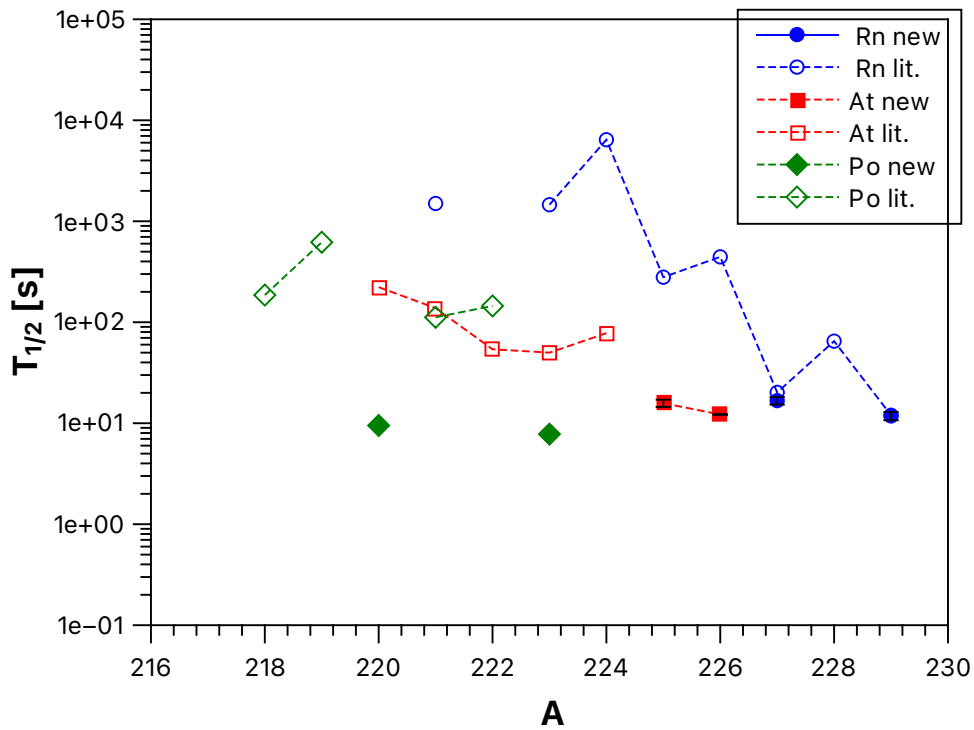


Ion	Q_{value} [MeV]	Experimental values [s]	
		Present work	Literature
$^{227}\text{Rn} \rightarrow ^{227}\text{Fr}$	1.32	16.7 ± 1.4	⁽¹⁾ 20.2 ± 0.4 (14)
$^{229}\text{Rn} \rightarrow ^{229}\text{Fr}$	1.87	11.8 ± 1.1	⁽²⁾ $12^{+1.2}_{-1.3}$ (15)
$^{225}\text{At} \rightarrow ^{225}\text{Rn}$	2.71	15.8 ± 1.3	-
$^{226}\text{At} \rightarrow ^{226}\text{Rn}$	1.22	12.2 ± 1.7	-
$^{220}\text{Po} \rightarrow ^{220}\text{At}$	0.88	9 ± 2	-
$^{223}\text{Po} \rightarrow ^{223}\text{At}$	3.65	7.8 ± 0.7	-

⁽¹⁾W. Kurcewicz et al., *Nucl. Phys. A* 621.4 (1997) 827–852

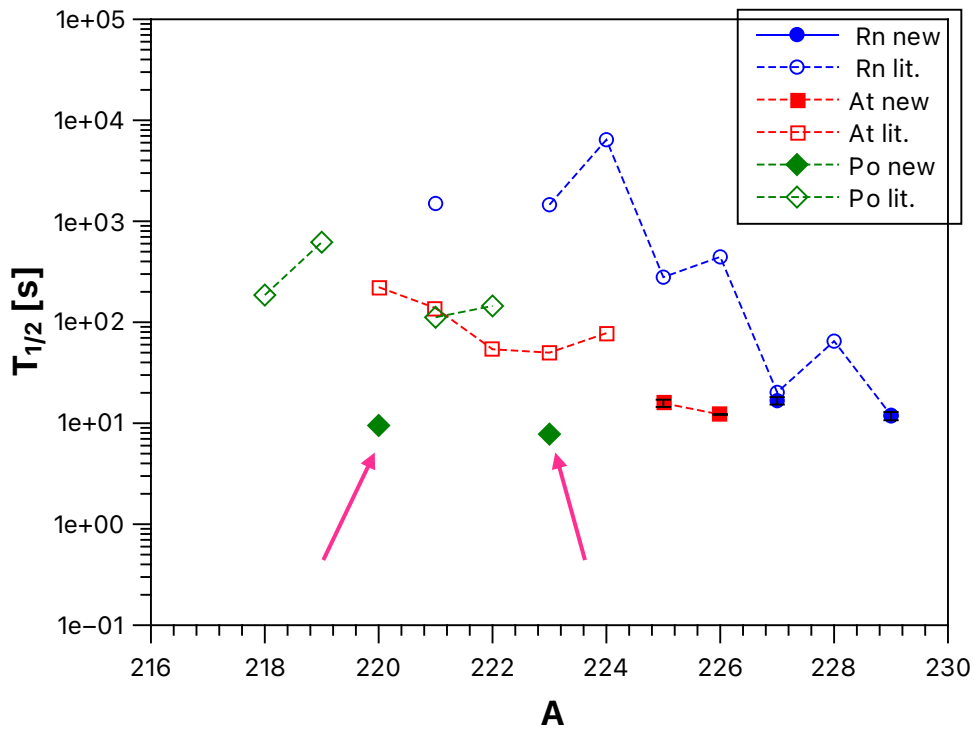
⁽²⁾D. Neidherr et al., *Phys. Rev. Lett.* 102 (2009) 112501

Results and comparison with literature data



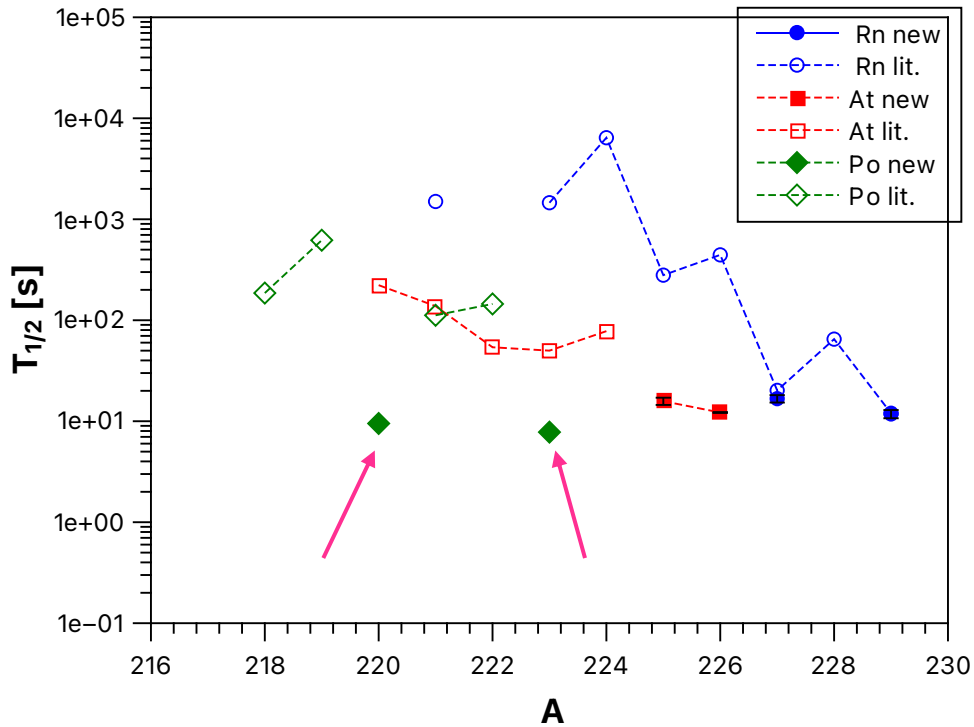
- Remeasured values agree with existing data
- Rn and At new data points follow general trend
- Pronounced odd-even staggering in Rn chain

Results and comparison with literature data

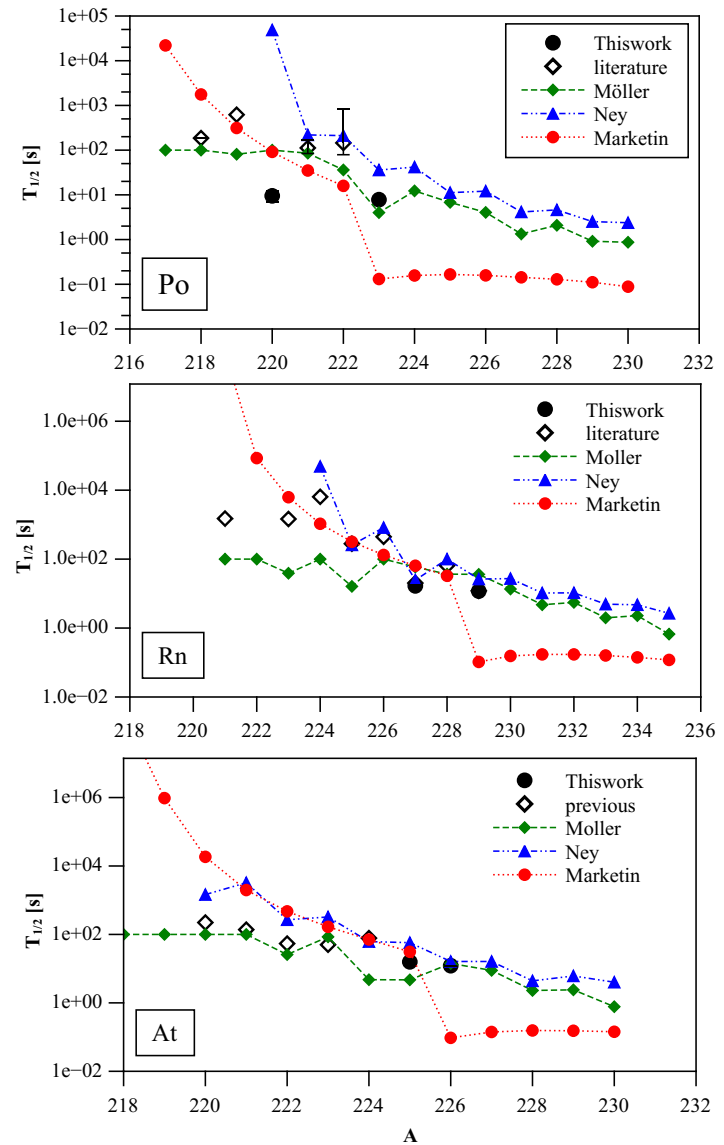


- Remeasured values agree with existing data
- Rn and At new data points follow general trend
- Pronounced odd-even staggering in Rn chain

Results and comparison with literature data



- Remeasured values agree with existing data
- Rn and At new data points follow general trend
- Pronounced odd-even staggering in Rn chain

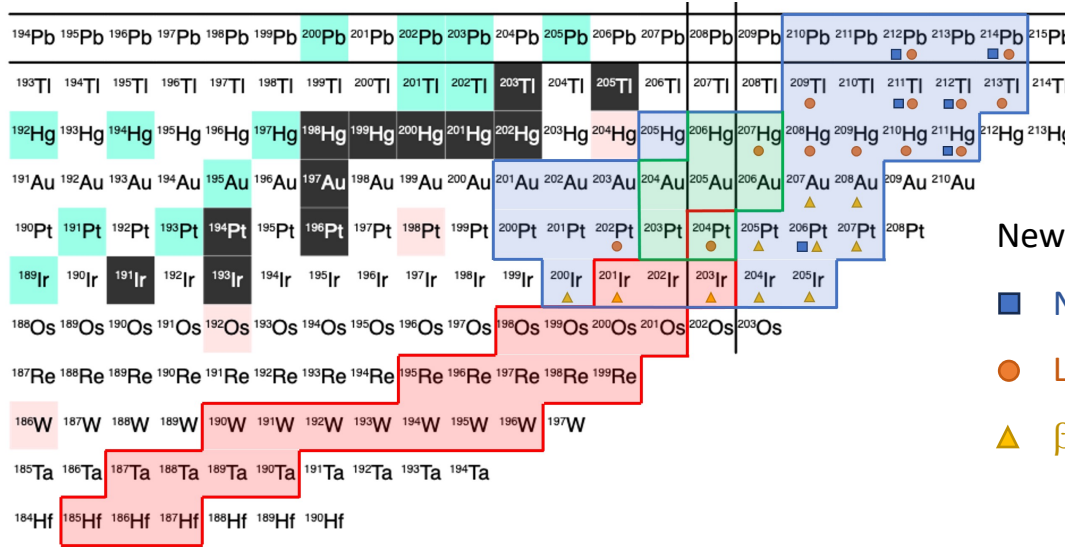


New experiment at GSI in June 2024

Spokepersons: M. Polettini, A. I. Morales

Main goals:

- ⇒ Obtain nuclear properties used as inputs into r-process network calculations
- ⇒ Provide new data to test nuclear models towards the N=126 waiting point



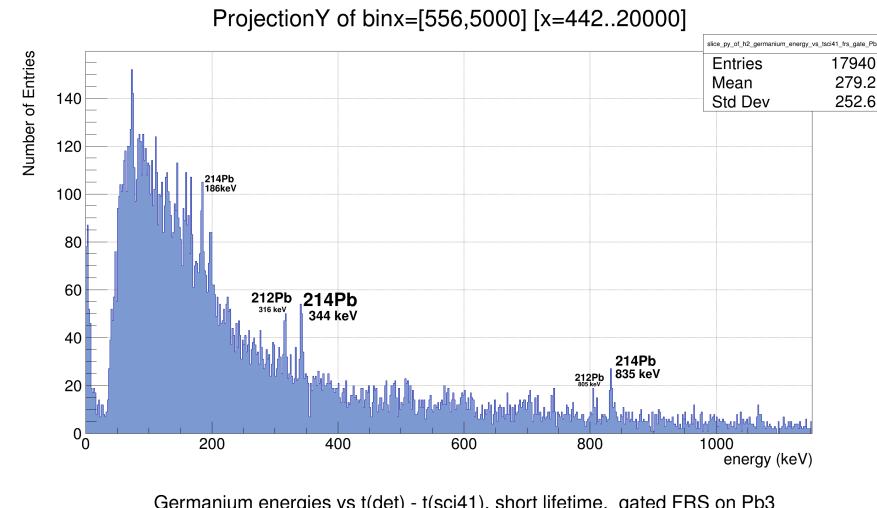
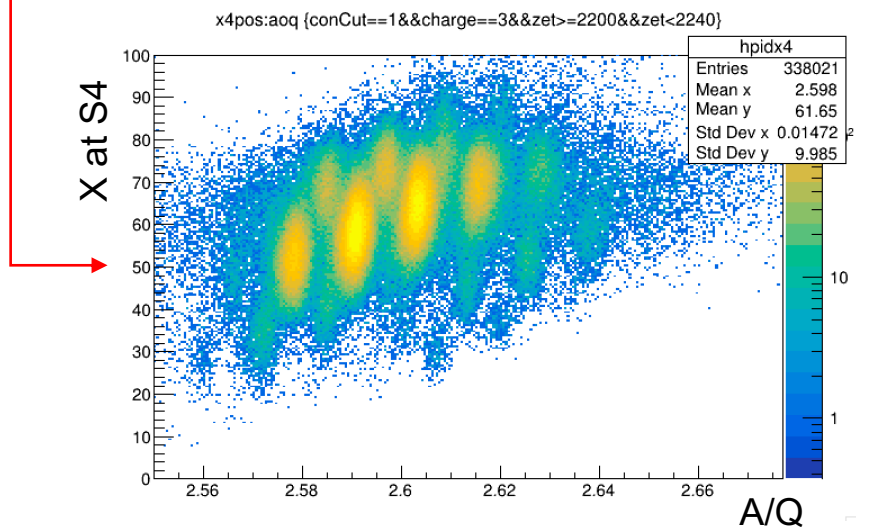
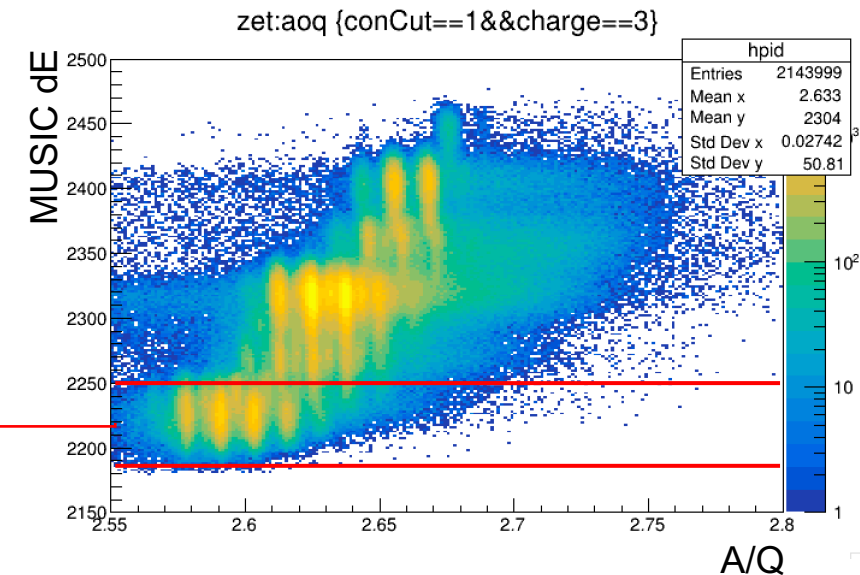
New experimental measurements on:

- New isomeric states
- Lifetime of low-lying states
- ▲ β-decay half-lives and spectroscopy

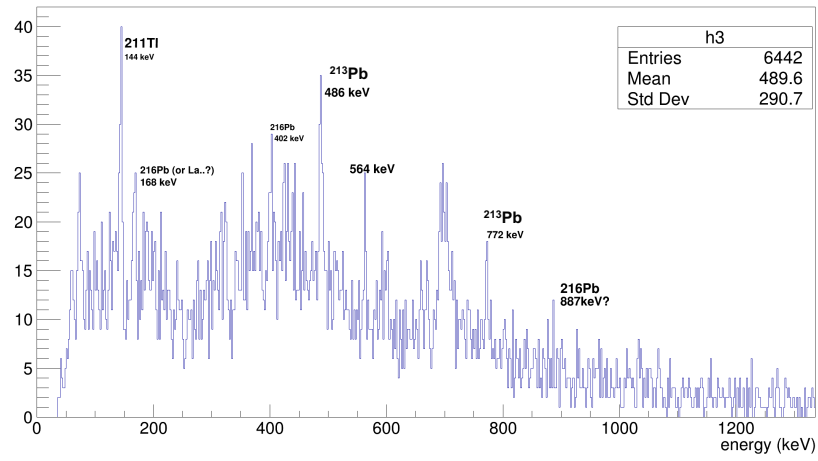
Focus on the Pt isotopic chain:

- Trace the evolution of **decay schemes** between N=122 and N=129
- Search for a **seniority isomer** in ^{206}Pt
- New **β-decay half-lives** measurements in $^{205,206,207}\text{Pt}$ and $^{207,208}\text{Au}$

New experiment: online results



Germanium energies vs t(det) - t(sci41), short lifetime, gated FRS on Pb3



Conclusions

β decay studies in the A~225 Po-Fr n-rich region and ^{100}Sn p-rich region. The experiments were performed at GSI in April 2021 using the FRS+DESPEC setup.

Obtained results:

- Study of low-lying states in $^{100,101,102}\text{Cd}$ via β -delayed spectroscopy and lifetime measurements in $^{98,100}\text{Cd}$
- New β -decay half-lives measured in $^{220,223}\text{Po}$, $^{225,226}\text{At}$, good agreement with previous measurements for $^{227,229}\text{Rn}$

Outlook:

- Two scientific papers and letters in preparation
- New experiment in N=126 region run in June 2024

The DESPEC collaboration for the S496 experiment

G. Zhang^{a,b}, M. Polettini^{a,b}, D. Mengoni^{a,b}, G. Benzonii^c, Z. Huang^{a,b}, M. Gorska^d, A. Blazhev^e, L. M. Fraile^f, A. Gargano^g, G. de Gregorio^g, F. Nowacki^h, H. M. Albers^d, A. Algoraiⁱ, S. Alhomaidhi^j, C. Appleton^k, T. Arici^d, M. Armstrong^e, A. Astier^l, A. Banerjee^d, D. Bazzacco^{a,b}, S. Bottoni^c, P. Boutachkov^d, A. Bracco^c, A. Bruce^m, D. Brugnara^{a,b}, F. Camera^c, B. Cederwallⁿ, M. Cicerchia^o, A. Corsi^p, M. L. Cortes^o, F.C.L. Crespi^c, T. Davidson^k, G. de Angelis^o, T. Dickel^d, A. Esmaylzadeh^e, F. Galtarossa^{a,b}, E. R. Gamba^c, J. Gerl^d, A. Goasdouff^o, A. Gottardo^o, A. Gozzelino^o, T. Grahn^q, J. Ha^{a,b}, E. Haettner^d, O. Hall^k, L. Harkness-Brennan^r, H. Heggen^d, N. Hubbard^j, A. Illana^q, P.R. Johni^j, J. Jolie^e, I. Kojouharov^d, N. Kurz^d, M. Labiche^s, S. M. Lenzi^{a,b}, S. Leoni^c, R. Lozeval^l, G. Mantovani^o, T. Marchio^o, H. Mayri^j, M. Mazzocco^{a,b}, R. Menegazzo^{a,b}, B. Million^c, A. K. Mistry^j, E. Nacheri^d, D. R. Napoli^o, R. Page^r, G. Pasqualato^{a,b}, J. Pellumajo^o, C. M. Petrache^l, R.M. Perez Vidal^o, N. Pietralla^j, Zs. Podolyák^t, A. Raggio^{a,b}, F. Recchia^{a,b}, P. H. Regan^t, J. M. Regis^e, P. Reiter^e, B. Rubio^l, M. Rudigier^j, P. Ruotsalainen^q, E. Sahin^j, H. Schaffner^d, Ch. Scheidenberger^d, L. Sexton^k, A. Sharma^d, M. Siciliano^u, J. Simpson^s, F. Soramel^{a,b}, T. Stetzi^j, J. J. Valiente-Dobon^o, J. Vesic^v, V. Werner^j, O. Wieland^c, P. Woods^k, A. Yaneva^d, I. Zanon^o, K. K. Zheng^l, R. Zidarovaj

^aUniversità degli Studi di Padova, Padova, 35131, Italy

^bINFN Sezione di Padova, Padova, 35131, Italy

^cINFN Sezione di Milano, Milano, 20133, Italy

^dGSI Helmholtzzentrum fur Schwerionenforschung, Darmstadt, 64291, Germany

^eInstitut fur Kernphysik, Universitat zu Koln, Cologne, 50937, Germany

^fGrupo de Fisica Nuclear and IPARCOS, Universidad Complutense de Madrid, Madrid, E-28040, Spain

^gIstituto Nazionale di Fisica Nucleare, Napoli, I-80126, Italy

^hUniversite de Strasbourg, IPHC, Strasbourg, 67037, France

ⁱInstituto de Fisica Corpuscular, CSIC-Universidad de Valencia, Valencia, E-46071, Spain

^jInstitut fur Kernphysik, Technische Universität Darmstadt, Darmstadt, 64289, Germany

^kSchool of Physics and Astronomy, University of Edinburgh, Edinburgh, H9 3FD, UK

^lUniversity Paris-Saclay, IJCLab, CNRS/IN2P3, Orsay, F-91405, France

^mSchool of Computing Engineering and Mathematics, University of Brighton, Brighton, BN2 4AT, UK

ⁿDepartment of Physics, KTH Royal Institute of Technology, Stockholm, SE-10691, Sweden

^oINFN Laboratori Nazionali di Legnaro, Legnaro, 35020, Italy

^pCEA-Saclay, IRFU/Service de Physique Nucleaire, Gif-sur-Yvette, 91191, France

^qUniversity of Jyvaskyla, Jyvaskyla, 40014, Finland

^rDepartment of Physics, Oliver Lodge Laboratory, University of Liverpool, Liverpool, L69 7ZE, UK

^sSTFC Daresbury Laboratory, Daresbury, WA4 4AD, UK

^tDepartment of Physics, University of Surrey, Surrey, GU2 7XH, UK

^uPhysics Division, Argonne National Laboratory, Argonne, IL 60439, USA

^vJozef Stefan Institute, Ljubljana, 1000, Slovenia

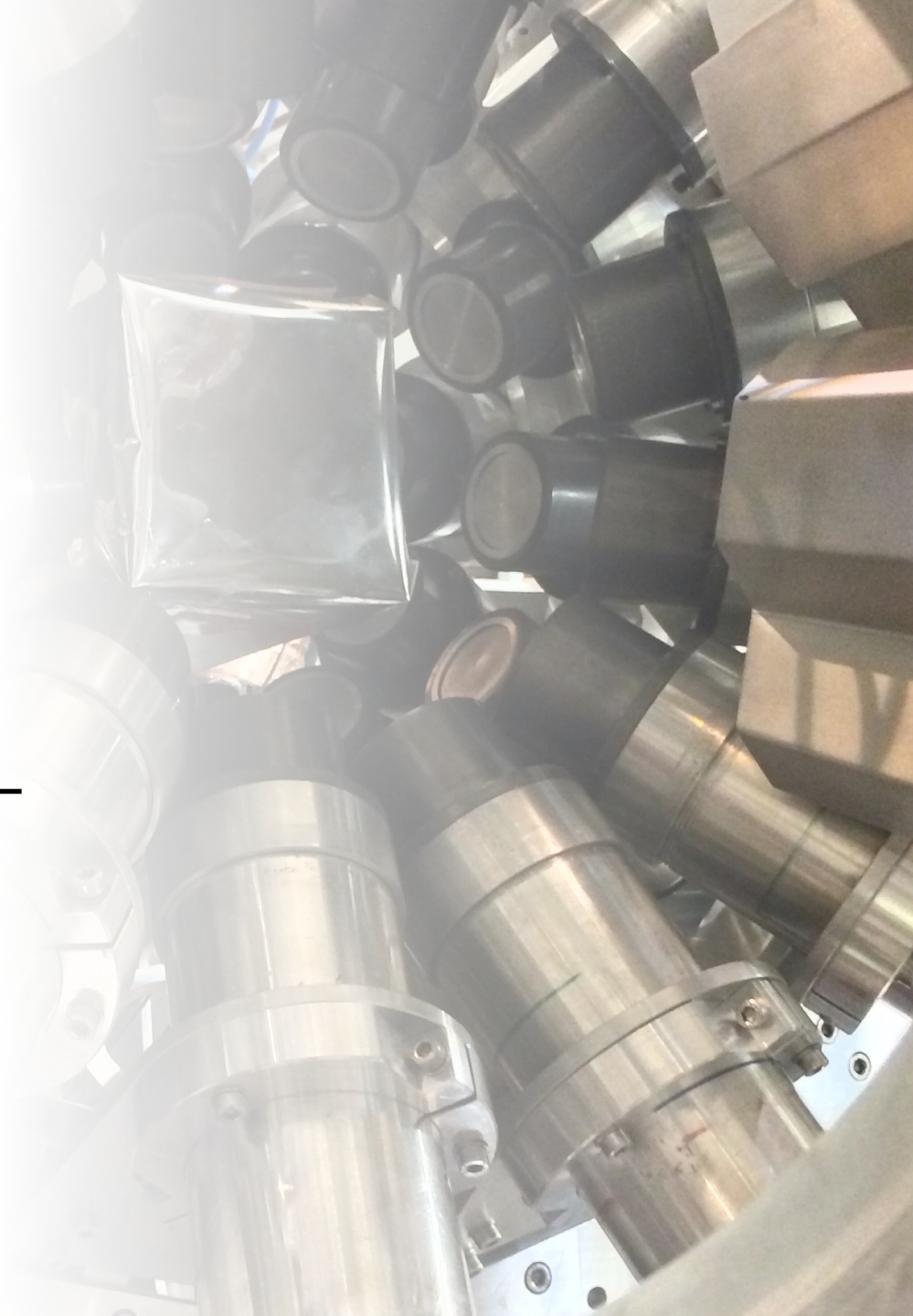
The DESPEC collaboration for the S460 experiment

M. Polettini^{(1)(*)}, G. Benzoni⁽¹⁾, J. Pellumai⁽²⁾⁽³⁾, J. J. Valiente-Dobón⁽³⁾, G. Zhang⁽⁴⁾, D. Mengoni⁽⁴⁾, R. M. Perez Vidal⁽³⁾, Z. Huang⁽⁴⁾, D. Genna⁽¹⁾, A. Bracco⁽¹⁾, G. Aggez⁽⁵⁾, U. Ahmed⁽⁶⁾, Ö. Aktas⁽⁷⁾, M. Al Aqueel⁽⁸⁾, B. Alayed⁽⁹⁾⁽¹⁰⁾, H. M. Albers⁽¹¹⁾, A. Algora⁽¹²⁾, S. Alhomaaidhi⁽¹¹⁾⁽⁶⁾, C. Appleton⁽¹³⁾, T. Arici⁽⁵⁾, M. Armstrong⁽¹⁴⁾, K. Arnswald⁽¹⁴⁾, M. Balogh⁽³⁾, A. Banerjee⁽¹¹⁾, J. Benito García⁽¹⁵⁾, A. Blazhev⁽¹⁴⁾, S. Bottoni⁽¹⁾, P. Boutachkov⁽¹¹⁾, A. Bruce⁽¹⁶⁾, C. Bruno⁽¹³⁾, F. Camera⁽¹⁾, B. Cederwall⁽⁷⁾, M. M. R. Chishti⁽¹⁷⁾, M. L. Cortés⁽⁶⁾, D. M. Cox⁽¹⁸⁾, F. C. L. Crespi⁽¹⁾, B. Das⁽⁷⁾, T. Davinson⁽¹³⁾, G. De Angelis⁽³⁾, T. Dickel⁽¹¹⁾, M. Doncel⁽¹⁹⁾, R. Donthi⁽²⁰⁾, A. Ertoprak⁽³⁾, R. Escudeiro⁽⁴⁾, A. Esmaylzadeh⁽¹⁴⁾, L. M. Fraile⁽¹⁵⁾, L. Gaffney⁽⁹⁾, E. R. Gamba⁽¹⁾, J. Gerl⁽¹¹⁾, M. Górska⁽¹¹⁾, A. Gottardo⁽³⁾, J. Ha⁽⁴⁾, E. Haettner⁽¹¹⁾, O. Hall⁽¹³⁾, H. Heggen⁽¹¹⁾, Y. Hrabar⁽¹⁸⁾, N. Hubbard⁽¹¹⁾⁽⁶⁾, S. Jazrawi⁽¹⁷⁾⁽²¹⁾, P. R. John⁽⁶⁾, J. Jolie⁽¹⁴⁾, C. Jones⁽¹⁶⁾, D. Joss⁽⁹⁾, D. Judson⁽⁹⁾, D. Kahl⁽²²⁾, V. Karayonchev⁽¹⁴⁾, E. Kazantseva⁽¹¹⁾, R. Kern⁽⁶⁾, L. Knafla⁽¹⁴⁾, I. Kojouharov⁽¹¹⁾, A. Korgul⁽²³⁾, W. Korten⁽²⁴⁾, P. Koseoglou⁽⁶⁾, G. Kosir⁽²⁵⁾, D. Kostyleva⁽¹¹⁾, T. Kurtukian-Nieto⁽²⁶⁾, N. Kurz⁽¹¹⁾, N. Kuzminchuk⁽¹¹⁾, M. Labiche⁽²⁷⁾, S. Lenzi⁽⁴⁾, S. Leoni⁽¹⁾, M. Llanos Expósito⁽¹⁵⁾, R. Lozeva⁽²⁸⁾, T. J. Mertzimekis⁽²⁹⁾, M. Mikolajczuk⁽²³⁾, B. Million⁽¹⁾, A. K. Mistry⁽¹¹⁾⁽⁶⁾, A. Morales⁽¹²⁾, I. Mukha⁽¹¹⁾, J. R. Murias⁽¹⁵⁾, D. Napoli⁽⁴⁾, B. S. Nara Singh⁽³⁰⁾, D. O'Donnell⁽³⁰⁾, S. E. A. Orrigo⁽¹²⁾, R. Page⁽⁹⁾, S. Pelonis⁽²⁹⁾, J. Petrovic⁽⁷⁾, N. Pietralla⁽⁶⁾, S. Pietri⁽¹¹⁾, S. Pigliapoco⁽⁴⁾, Zs. Podolyak⁽¹⁷⁾, C. Porzio⁽¹⁾, B. Quintana Arnes⁽³¹⁾, F. Recchia⁽⁴⁾, P. H. Regan⁽¹⁷⁾⁽²¹⁾, J.-M. Régis⁽¹⁴⁾, P. Reiter⁽¹⁴⁾, K. Rezynkina⁽⁴⁾, P. Roy⁽³²⁾⁽¹¹⁾, M. Rudigier⁽⁶⁾, P. Ruotsalainen⁽³³⁾, E. Sahin⁽¹¹⁾⁽⁶⁾, L. G. Sarmiento⁽¹⁸⁾, M.-M. Satrazani⁽⁹⁾, H. Schaffner⁽¹¹⁾, C. Scheidenberger⁽¹¹⁾, L. Sexton⁽¹³⁾, A. Sharma⁽³⁴⁾, J. Smallcombe⁽⁹⁾, P.-A. Söderström⁽²²⁾, A. Sood⁽⁷⁾, P. Vasileiou⁽²⁹⁾, J. Vesic⁽²⁵⁾, J. Vilhena⁽³⁵⁾, L. Waring⁽⁹⁾, H. Weick⁽¹¹⁾, V. Werner⁽⁶⁾, J. Wiederhold⁽⁶⁾, O. Wieland⁽¹⁾, K. Wimmer⁽¹¹⁾, H. J. Wollersheim⁽¹¹⁾, P. Woods⁽¹³⁾, A. Yaneva⁽¹⁴⁾, I. Zanon⁽²⁾⁽³⁾, J. Zhao⁽¹¹⁾, R. Zidarova⁽⁶⁾, S. Ziliani⁽¹⁾, G. Zimba⁽³³⁾ and A. Zyriiou⁽²⁹⁾

⁽¹⁾ Dipartimento di Fisica, Università degli Studi di Milano and INFN Milano - Milan, Italy, ⁽²⁾ Dipartimento di Fisica e Scienze della Terra, Università di Ferrara - Ferrara, Italy, ⁽³⁾ INFN, Laboratori Nazionali di Legnaro - Legnaro, Italy, ⁽⁴⁾ Dipartimento di Fisica e Astronomia, Università di Padova and INFN Padova - Padua, Italy, ⁽⁵⁾ Istanbul University, Graduate School of Sciences, Department of Physics - Istanbul, Turkey, ⁽⁶⁾ Institut für Kernphysik, Technische Universität Darmstadt - Darmstadt, Germany, ⁽⁷⁾ KTH Royal Institute of Technology - Stockholm, Sweden, ⁽⁸⁾ Imam Mohammad Ibn Saud Islamic University - Riyadh, Saudi Arabia, ⁽⁹⁾ Department of Physics, Oliver Lodge Laboratory, University of Liverpool - Liverpool, UK, ⁽¹⁰⁾ Ar Rass College of Sciences and Arts, Qassim University - Quassim, Saudi Arabia, ⁽¹¹⁾ GSI Helmholtzzentrum für Schwerionenforschung GmbH - Darmstadt, Germany, ⁽¹²⁾ Instituto de Fisica Corpuscular, CSIC-Universidad de Valencia - Valencia, Spain, ⁽¹³⁾ University of Edinburgh, School of Physics and Astronomy - Edinburgh, UK, ⁽¹⁴⁾ Institut für Kernphysik der Universität zu Köln - Köln, Germany, ⁽¹⁵⁾ Grupo de Física Nuclear and IPARCOS, Universidad Complutense de Madrid - Madrid, Spain, ⁽¹⁶⁾ School of Computing Engineering and Mathematics, University of Brighton Brighton, UK, ⁽¹⁷⁾ Department of Physics, University of Surrey - Guildford, UK, ⁽¹⁸⁾ Department of Physics, Lund University - Lund, Sweden, ⁽¹⁹⁾ Department of Physics, University of Stockholm - Stockholm, Sweden, ⁽²⁰⁾ Department of Nuclear and Atomic Physics, Tata Institute of Fundamental Research, Mumbai, India, ⁽²¹⁾ National Physical Laboratory - Teddington, UK, ⁽²²⁾ ELI-NP Center for Extreme Light Infrastructure, Nuclear Physics - Magurele, Romania, ⁽²³⁾ Department of Physics, University of Warsaw - Warsaw, Poland, ⁽²⁴⁾ Irfu, CEA, Université Paris-Saclay - Paris-Saclay, France, ⁽²⁵⁾ Jozef Stefan Institute - Ljubljana, Slovenia, ⁽²⁶⁾ CENBG, Université de Bordeaux, CNRS/IN2P3 - Bordeaux, France, ⁽²⁷⁾ STFC, Daresbury Laboratory - Daresbury, UK, ⁽²⁸⁾ Université Paris-Saclay, IJCLab, CNRS/IN2P3 - Paris-Saclay, France, ⁽²⁹⁾ National and Kapodistrian University of Athens - Athens, Greece, ⁽³⁰⁾ School of Computing, Engineering and Physical Sciences, University of West Scotland, Glasgow, UK, ⁽³¹⁾ Laboratorio de Radiaciones Ionizantes, Universidad de Salamanca - Salamanca, Spain, ⁽³²⁾ Variable Energy Cyclotron Centre - 1/AF Bidhan Nagar, Kolkata, India, ⁽³³⁾ University of Jyväskylä - Jyväskylä, Finland, ⁽³⁴⁾ Department of Physics, Indian Institute of Technology Ropar - Ropar, India, ⁽³⁵⁾ LPMCN, Université de Lyon - Lyon, France



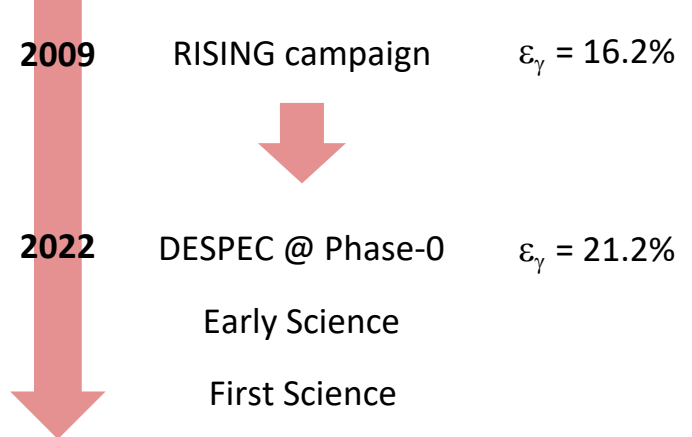
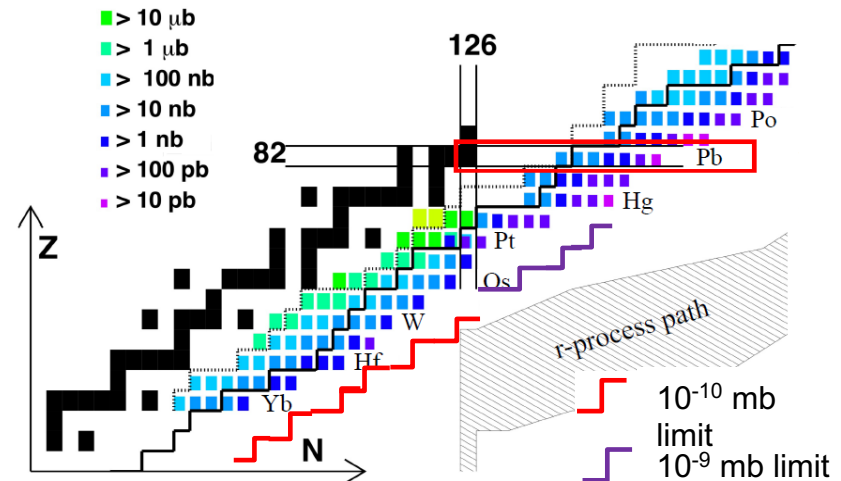
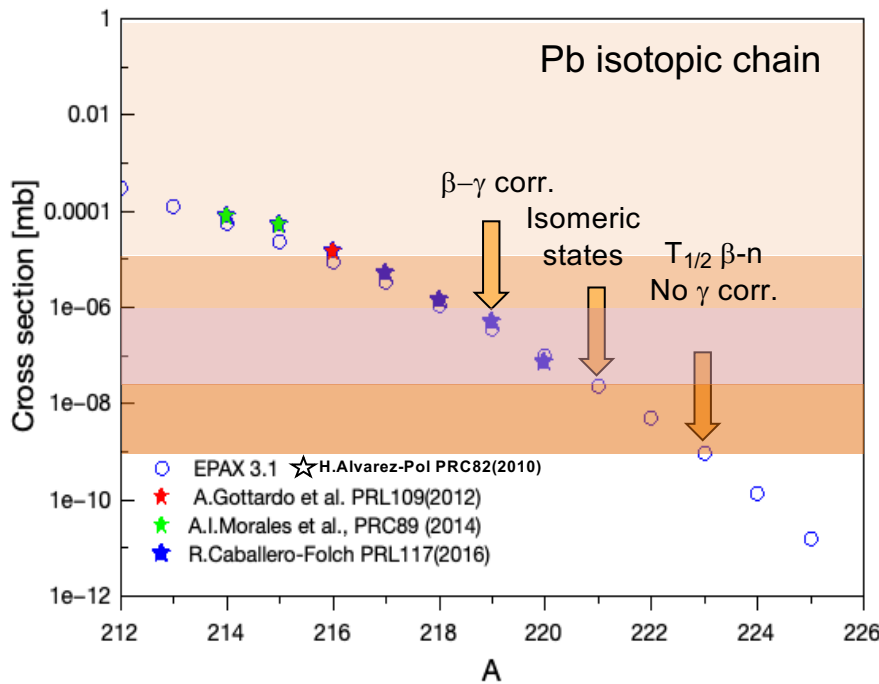
Thank you for your attention!



A quest towards the *r*-process waiting point

Answering to fundamental questions:

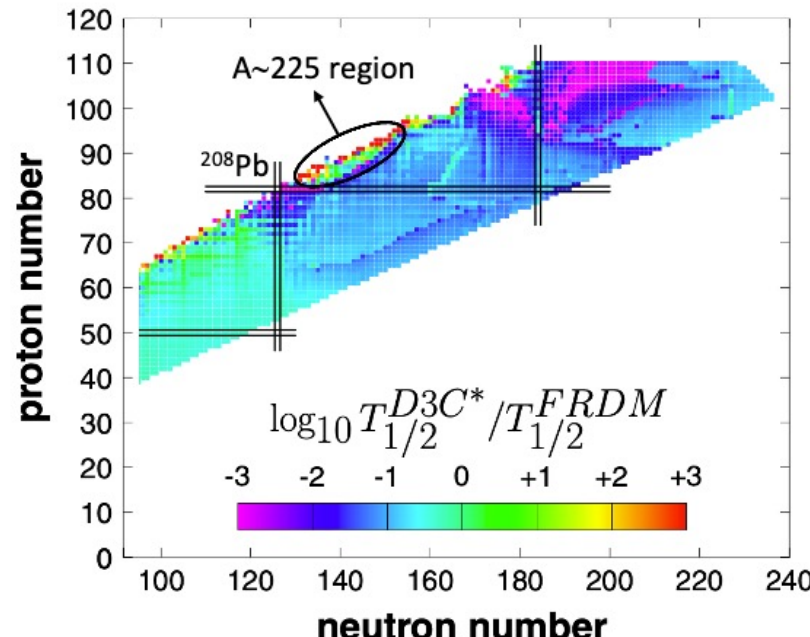
- **Exact location** of *r*-process path for heavy elements
- Role of **first-forbidden β -decay**
- Role of **delayed-neutron emission**
- **Fission recycling**



- Increasing primary beam intensity
- Improved γ efficiency
- Faster DAQ
- Improved FRS transmission

Nuclear physics inputs

- Key quantities in nucleosynthesis calculations:
 - nuclear masses → M_n, Q_β
 - decay rates → beta and alpha lifetimes τ_α, τ_β
 - β -delayed neutron emission → P_n
 - neutron capture rates → $\sigma(n, \gamma), \sigma(\gamma, n)$
 - fission probabilities

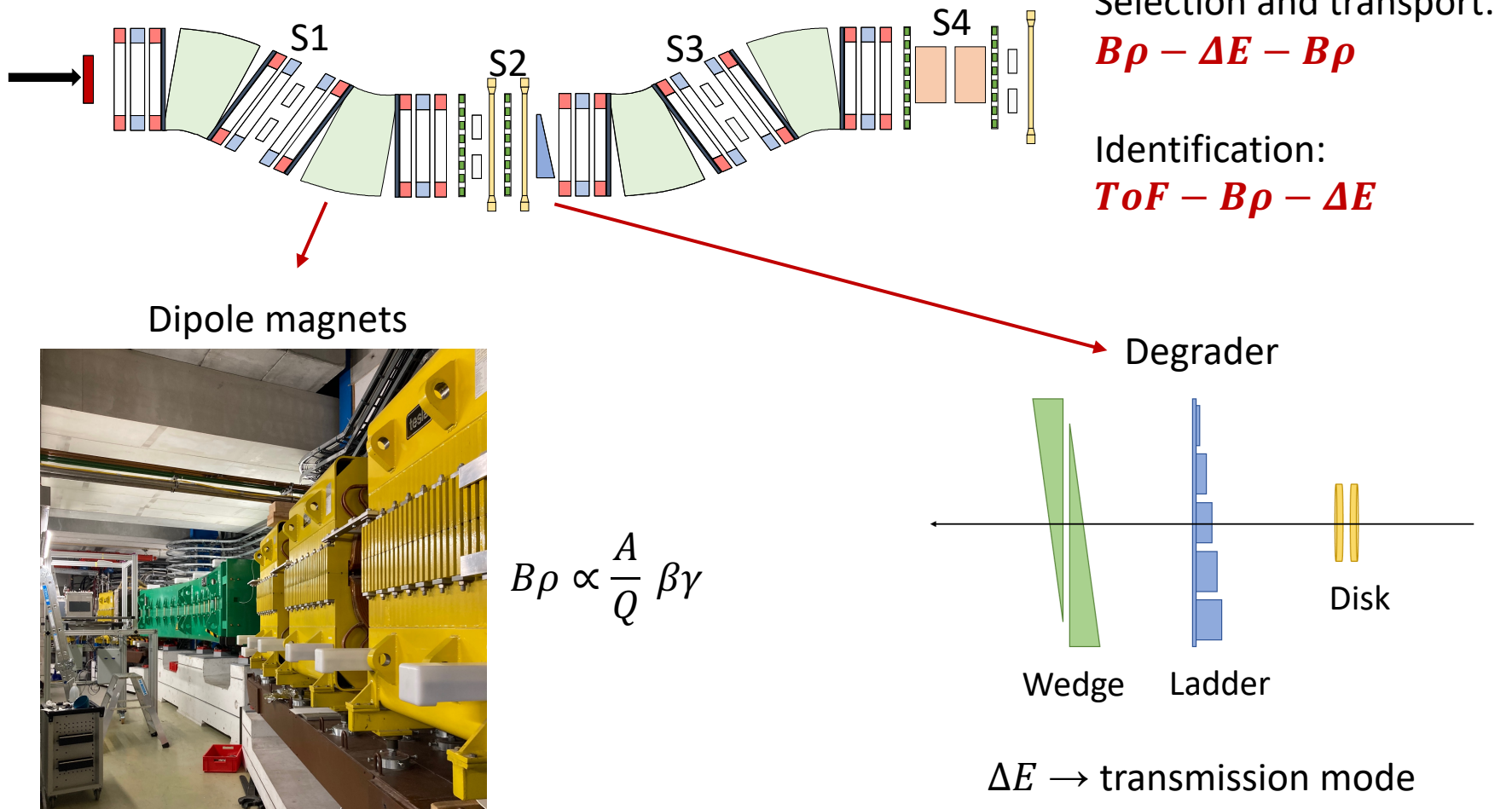


T. Marketin et al., Phys. Rev. C 93 (2016) 025805

Theoretical models show deviations in heavy n-rich nuclei

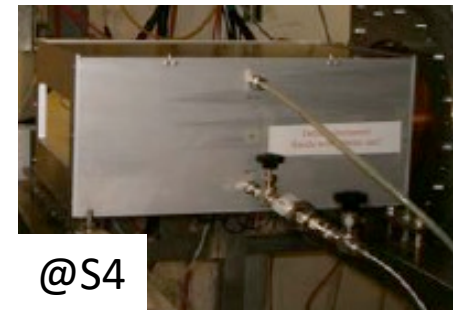
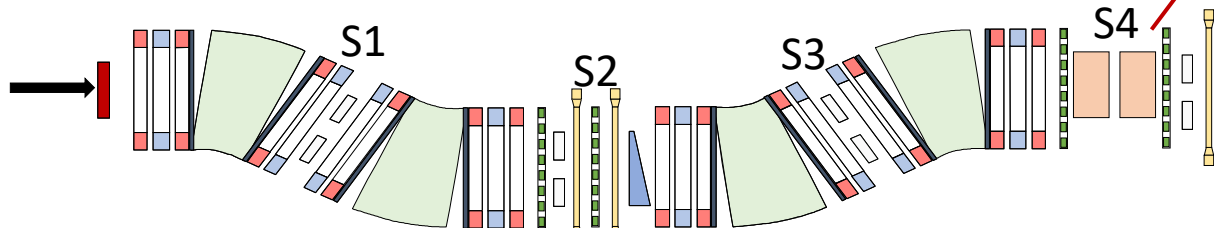
→ Need for β -decay half-lives measurements in the $N > 126$ region

The FRS magnetic spectrometer

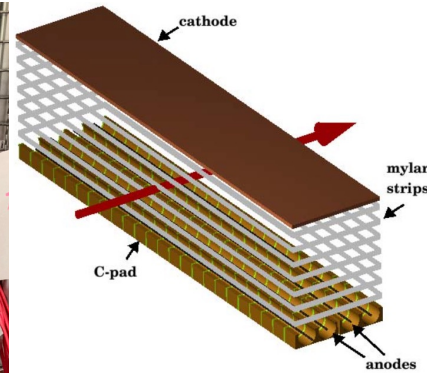


Ion identification

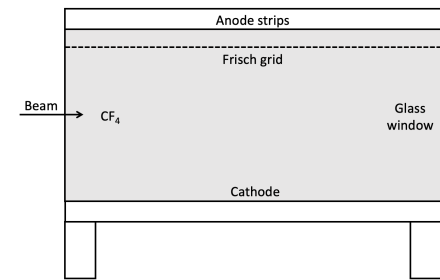
Multi Sampling Ionisation Chambers (MUSIC)



Time Projection Chamber (TPC)



Plastic scintillators



↓

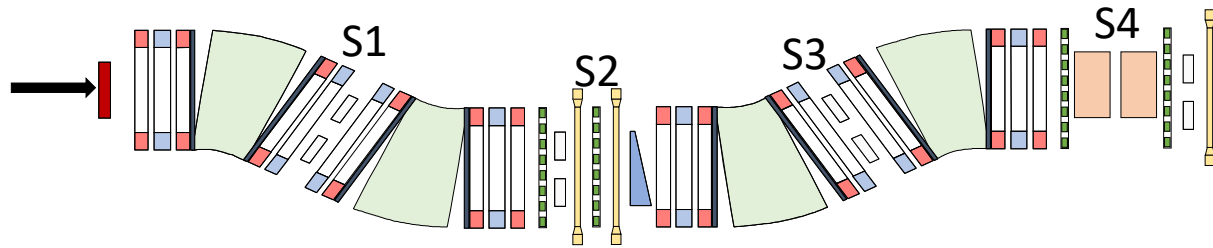
Z

$$\Delta E \propto Z^2 f(\beta)$$

A/Q

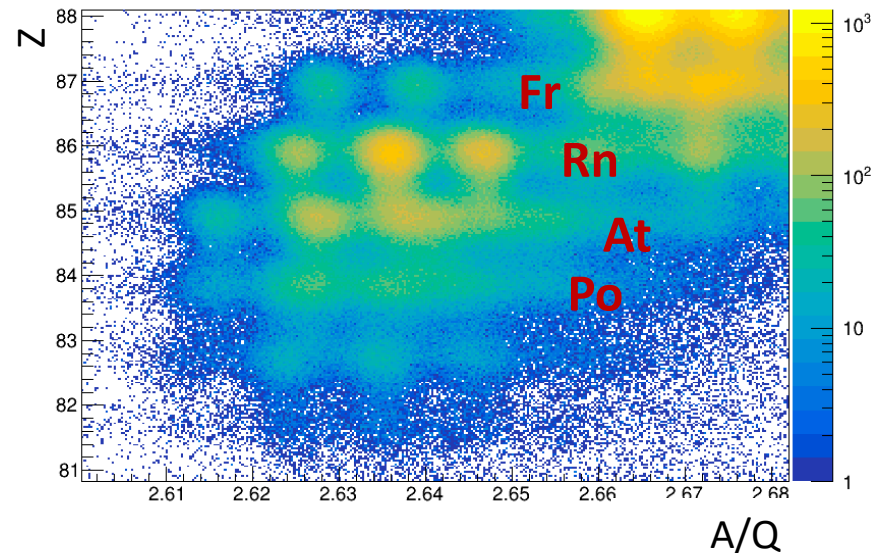
$$\frac{A}{Q} = \frac{B\rho}{\beta\gamma}$$

Ion identification

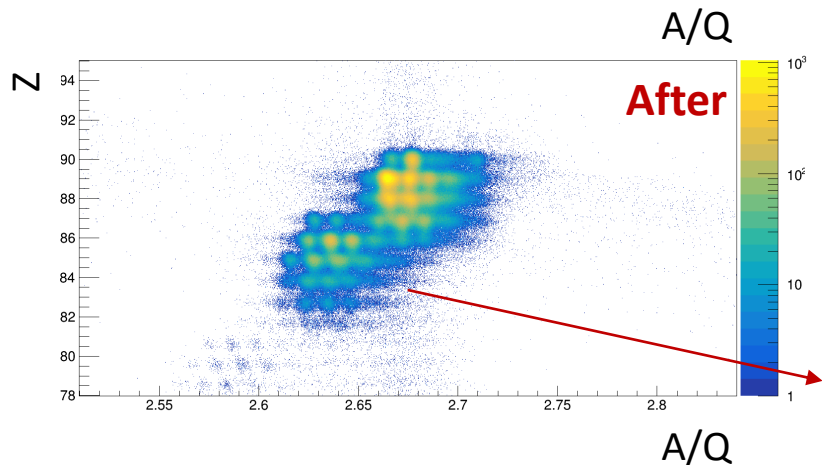
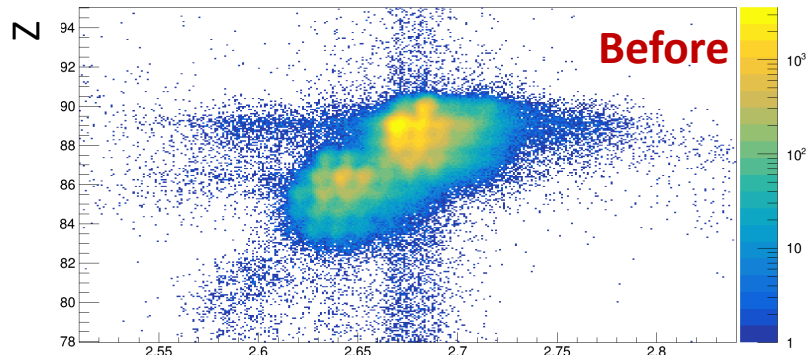


ID plot produced via the measurement of:

- The ratio of **mass number over ionic charge**
 A/Q
- The **atomic number Z** or the **X position** in the focal planes

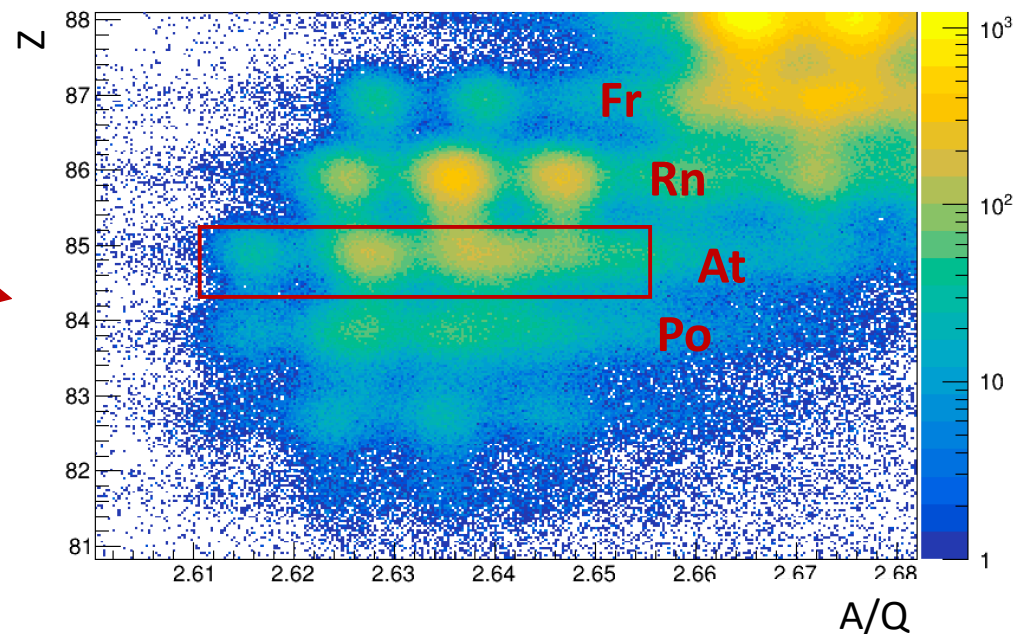


Identification plot

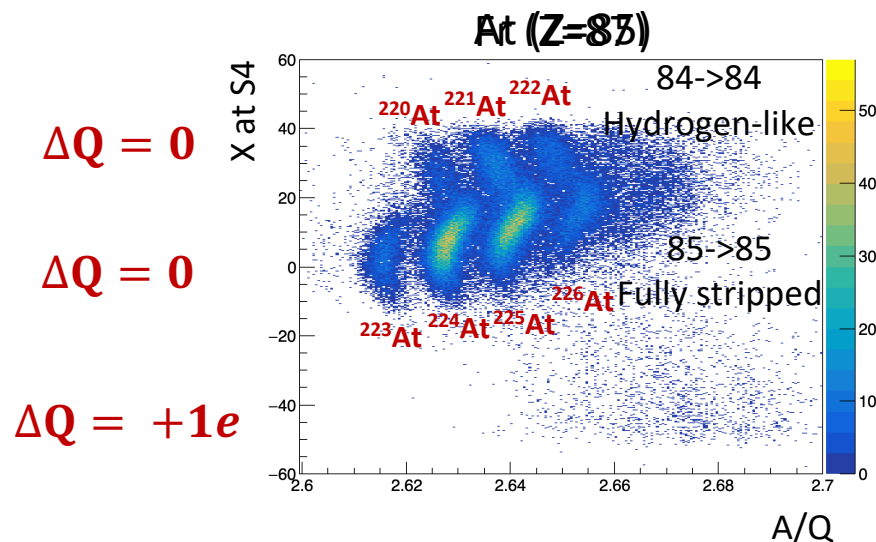
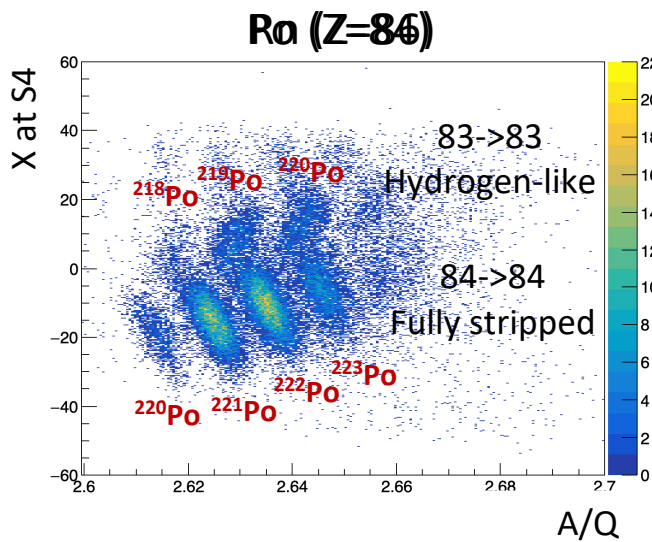
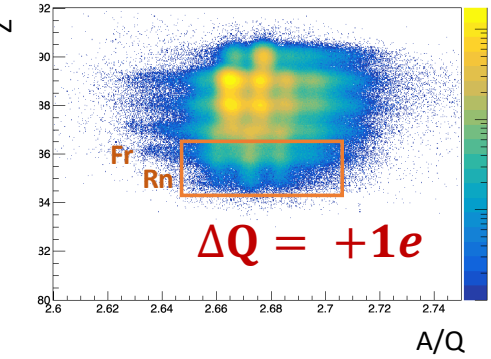
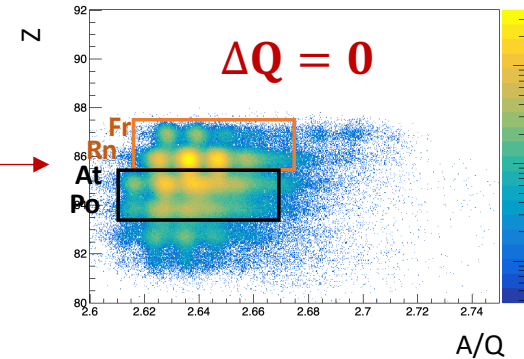
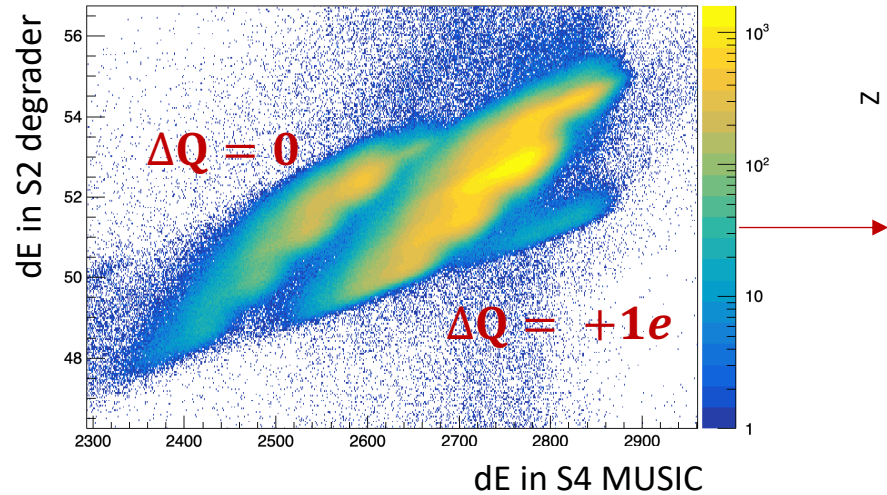


A/Q resolution improvement: $\sim 30\%$

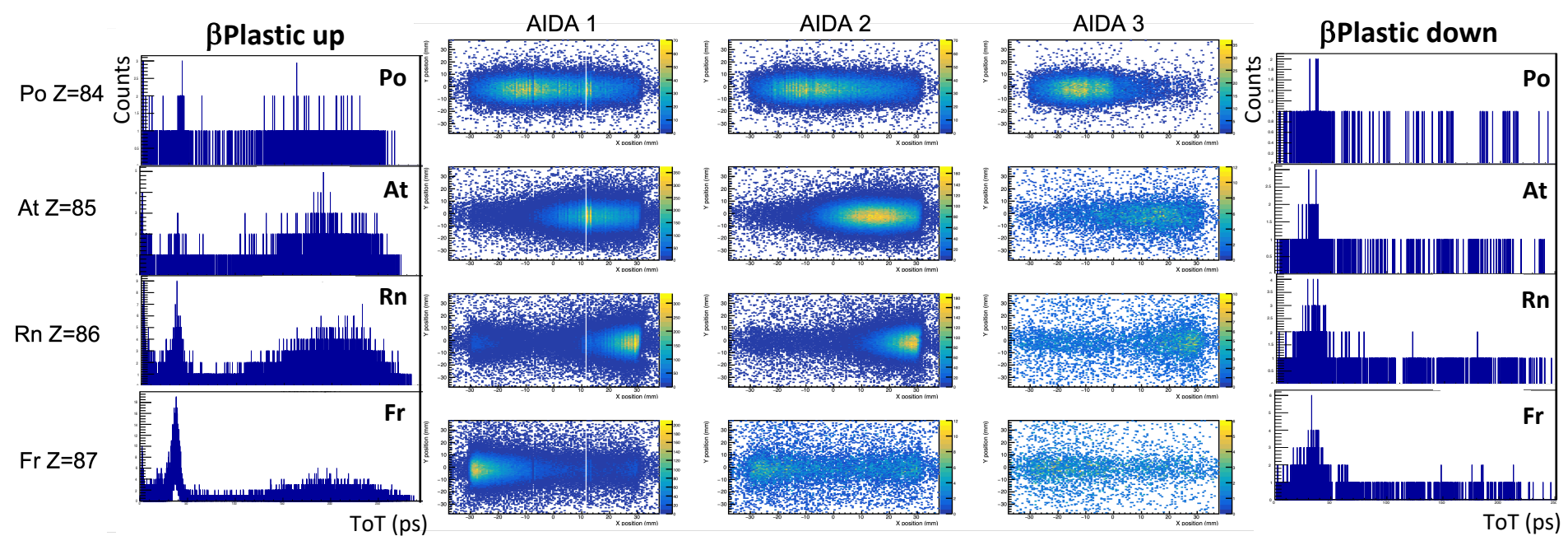
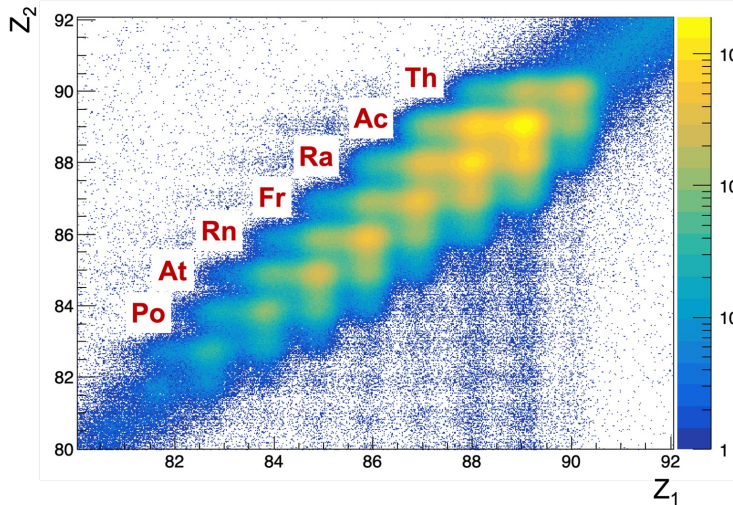
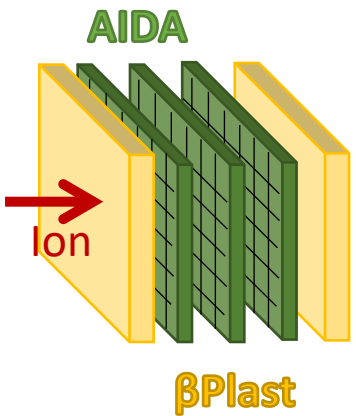
- ✓ ToF and MUSIC calibration
- ✓ Position calibration
- ✓ Gain drift correction
- ✓ Angle correction at S2 and S4



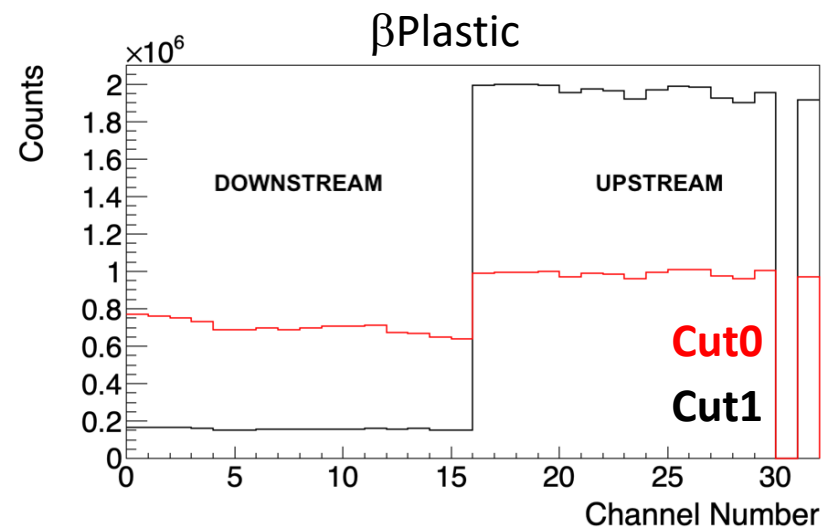
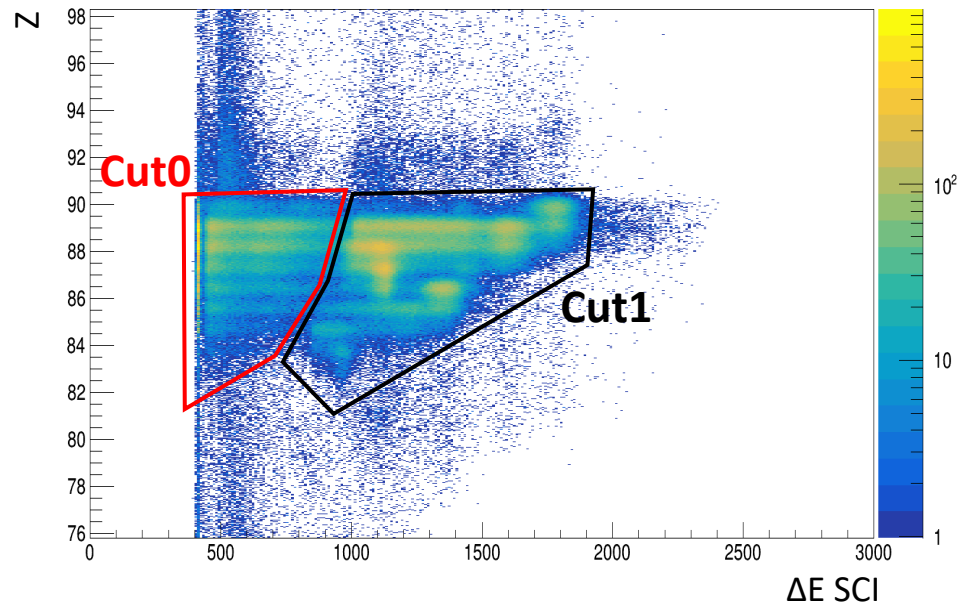
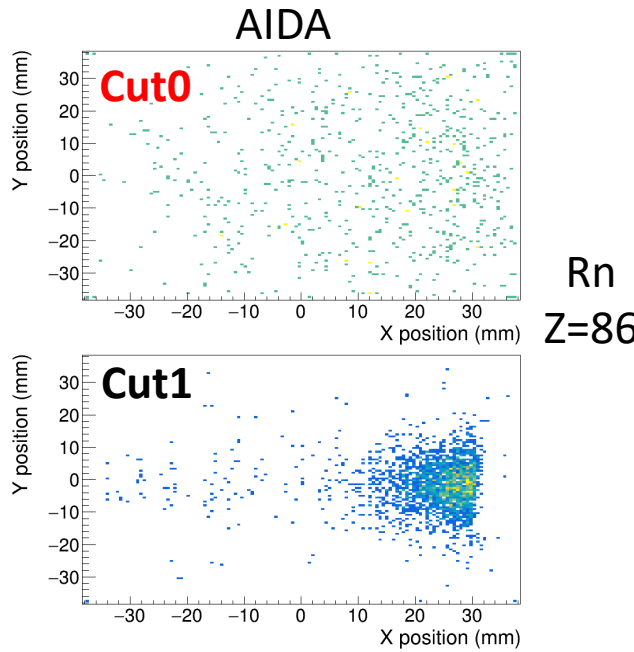
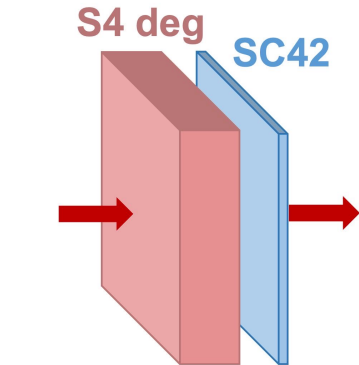
FRS analysis: study of charge states



Implantation profile

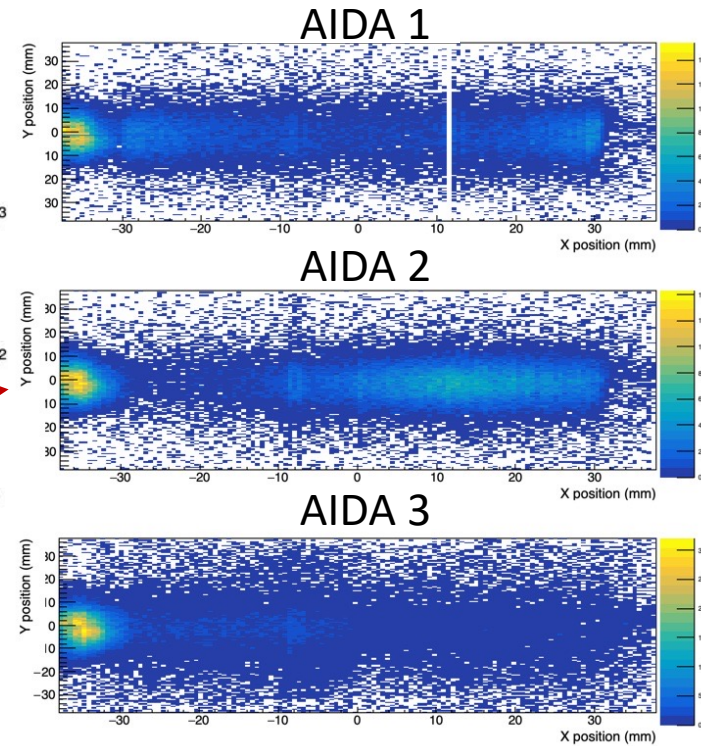
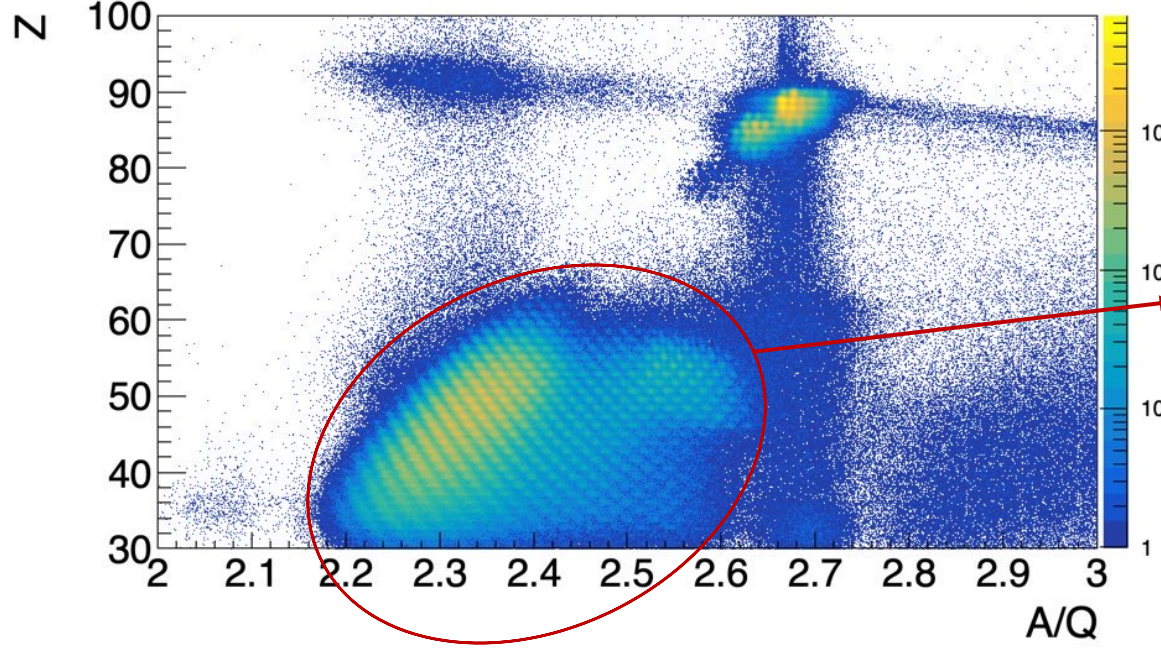


Secondary reactions in S4 degrader

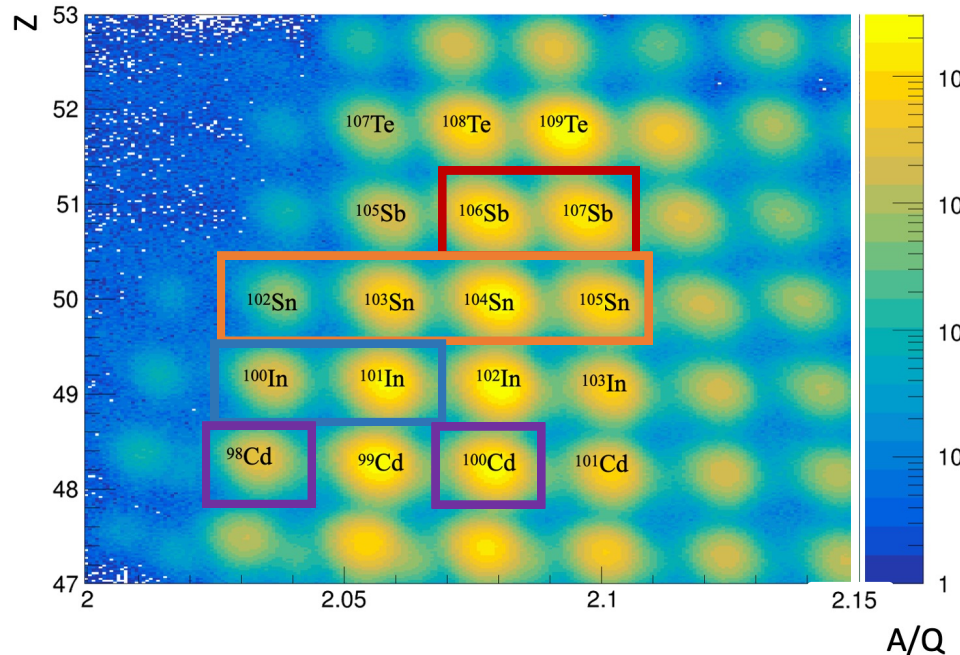


Fission fragments contribution

- Implantation rate: $\sim 10^3$ pps per detector
- Fission fragments contribution: $\sim 90\%$



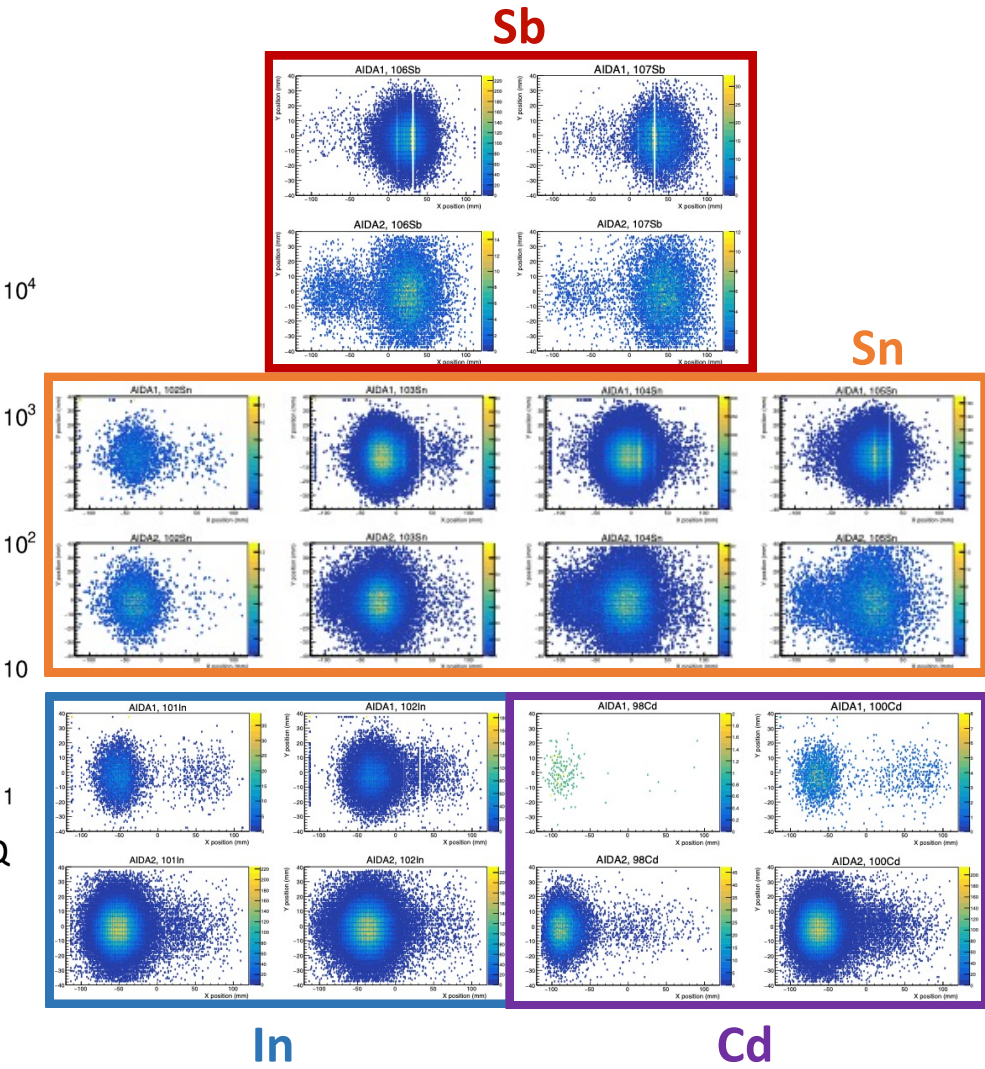
ID plot for Dataset2



Not-fully achromatic mode



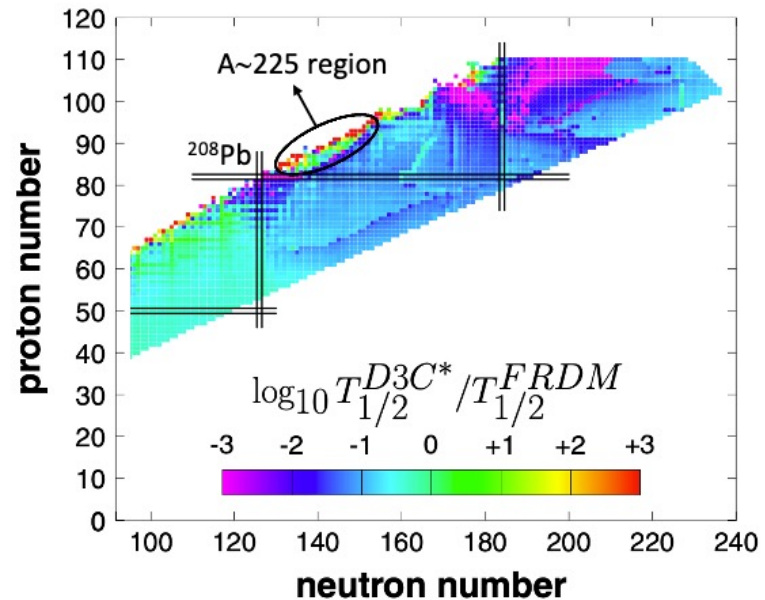
High overlap in implantation



Available theoretical models

Global models providing full β -decay tables for n-rich isotopes:

- P. Möller et al. (2019)
 - ground state masses based on FRDM,
 - β -decay half-lives determined from QRPA
- T. Marketin et al. (2016)
 - self consistent, microscopic description based on RHB
 - even ground states computed for odd-A and odd-odd nuclei
- E. M. Ney et al. (2020)
 - microscopic description based on a global Skyrme density functional
 - Equal filling approximation applied to describe odd-A and odd-odd nuclei

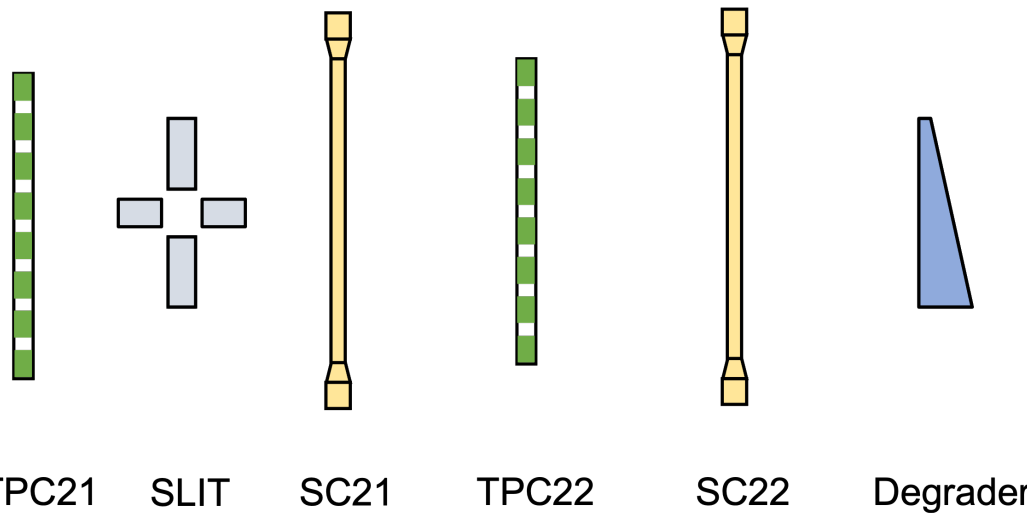


T. Marketin et al., Phys. Rev. C 93 (2016) 025805

Small error in Q -value
→ large effect on the $T_{1/2}$

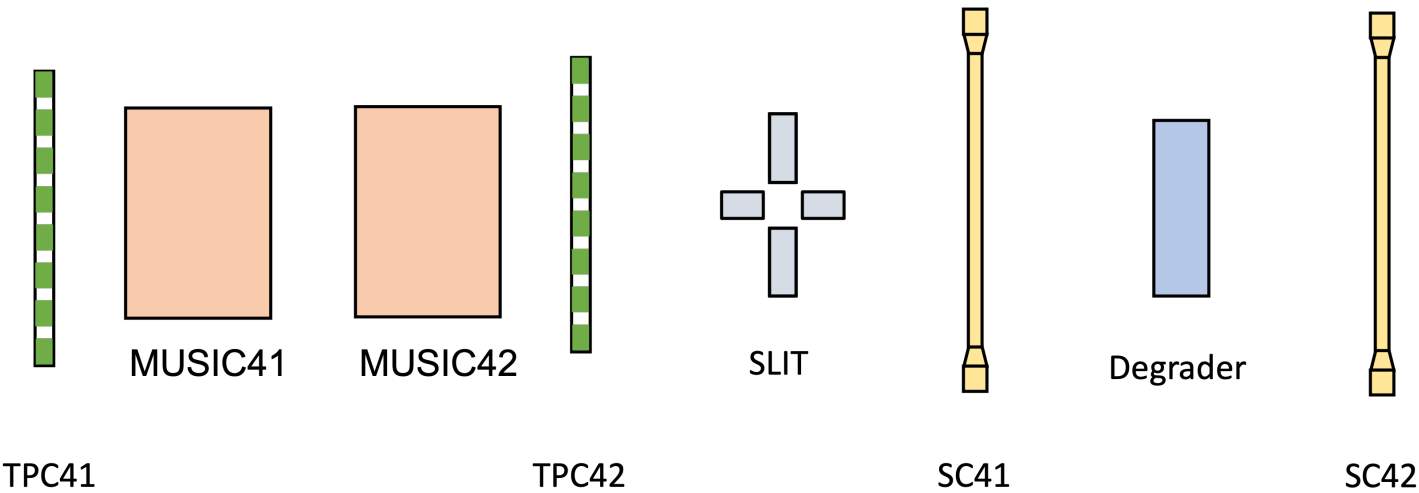
$$T_{1/2} \propto \frac{1}{S_\beta (Q_\beta - E^*)^5}$$

The S2 detectors



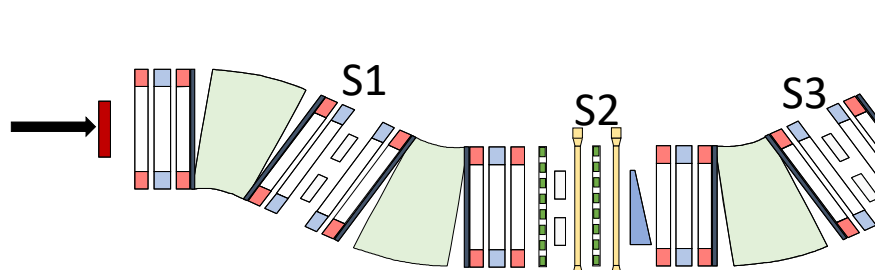
- 2 TPC detectors for position measurements
- 2 scintillators for TOF determination
- XY slits
- Degrader wedge

The S4 detectors



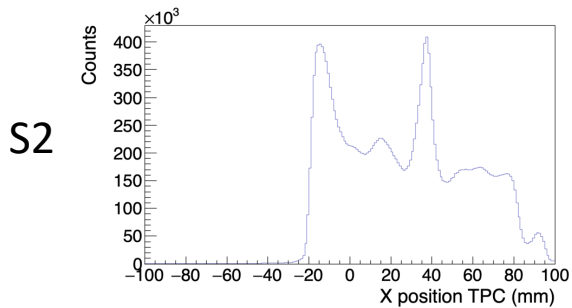
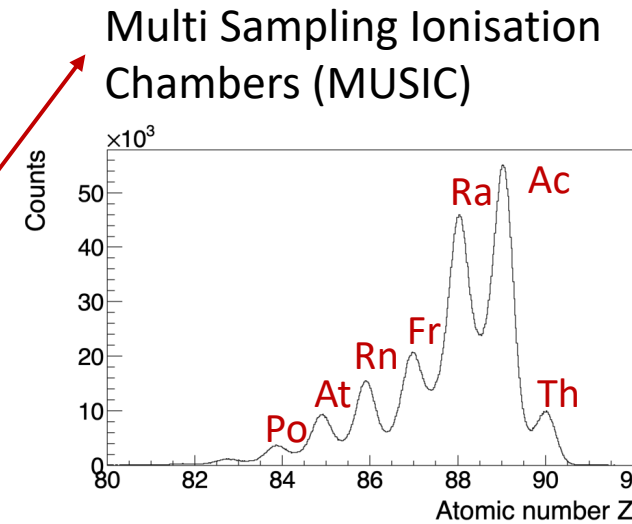
- 2 TPC detectors for position measurements
- 2 MUSIC detector for Z measurements
- XY slits
- 2 scintillators for TOF determination
- Degrader

Detectors along FRS

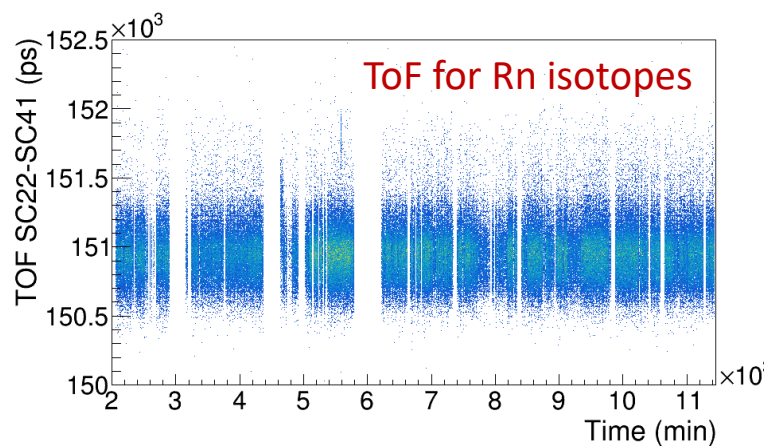
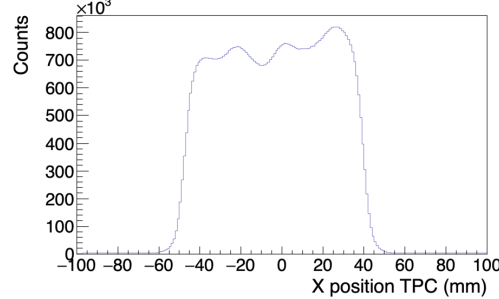


Time Projection Chamber (TPC)

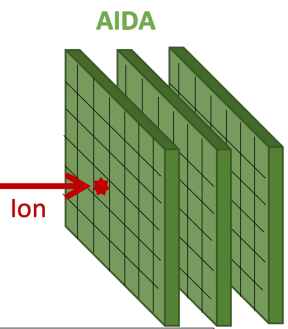
Plastic scintillators



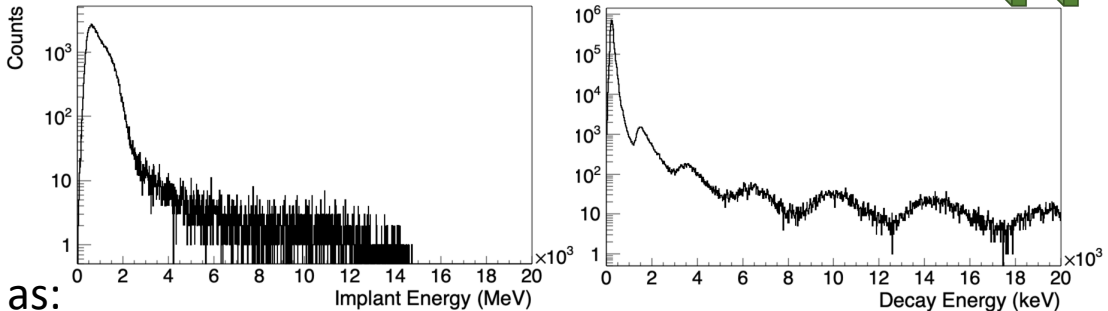
S4



The AIDA detector

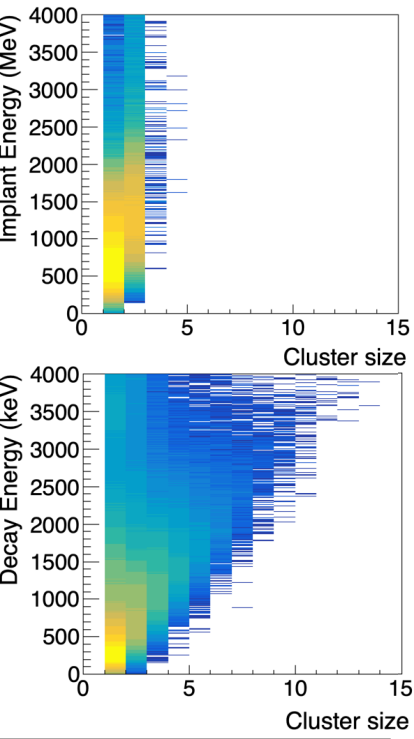


DSSD tiles: 8 cm x 8 cm, 1 mm thick, 0.056 mm pitch



Data organised as:

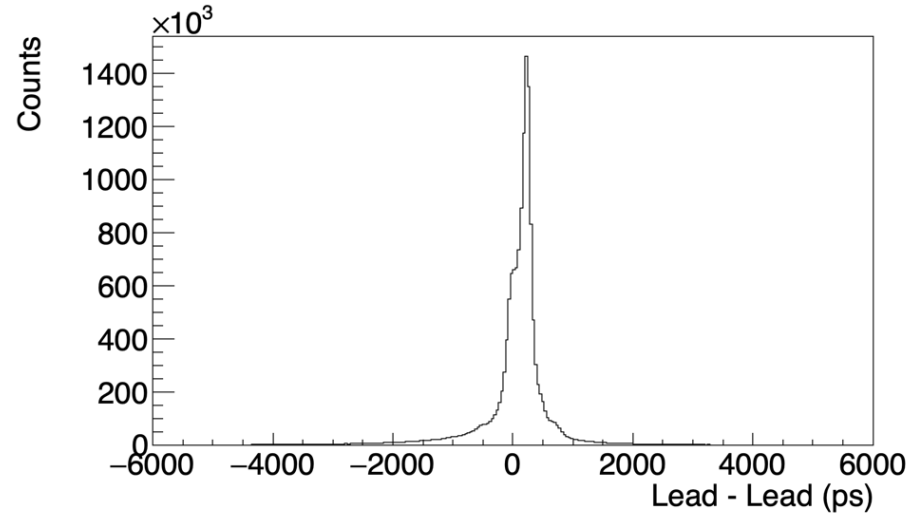
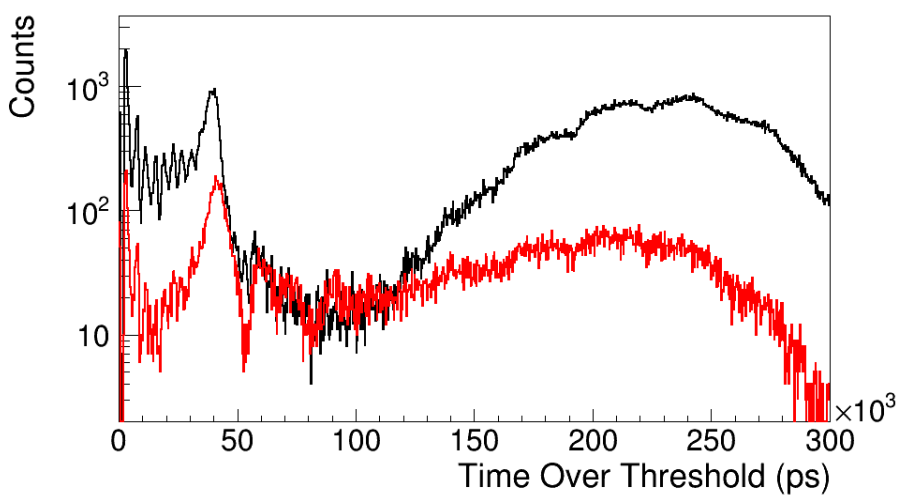
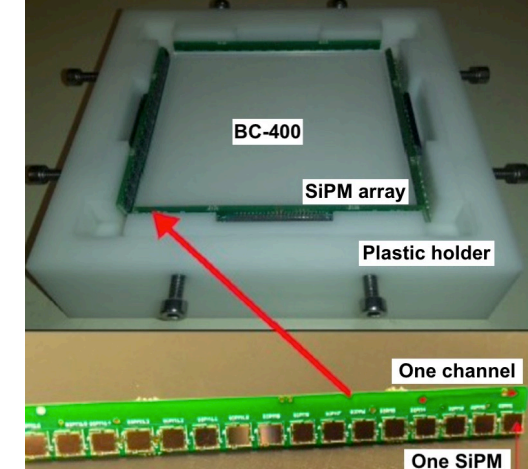
- Event number
- DSSD layer number,
- Strip X,Y
- Position X,Y in mm
- Energy (MeV for implants, keV for decays)
- Energy X,Y
- Cluster size X,Y
- Time (10 ns precision for implants, 2 μ s for decays)
- Time X,Y
- Fast time (10 ns precision for implants and decays)
- Stopped (if the implant is stopped in the DSSD)



The β Plastic detector

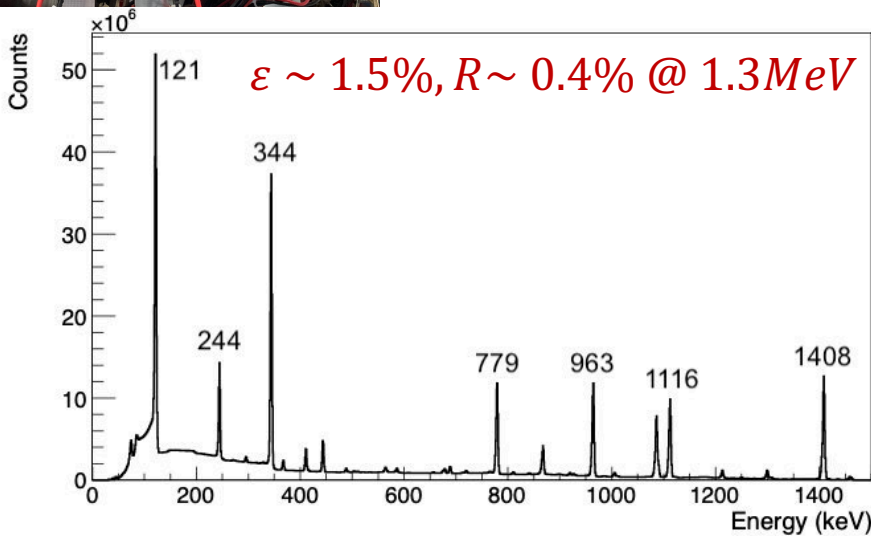
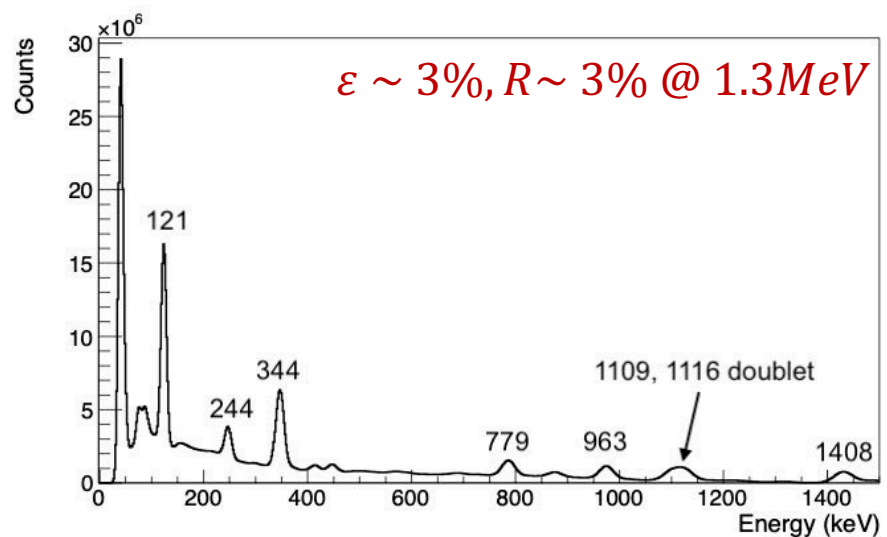
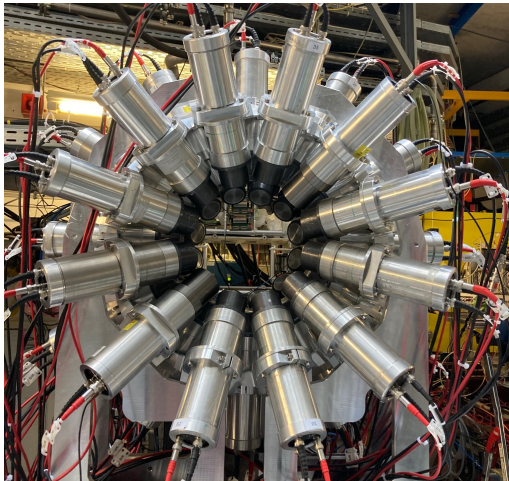
Two 3mm thick plastic scintillator coupled to SiPMs

- Energy info conveyed by a time over threshold spectrum
- Timing measurements as time difference between two channels

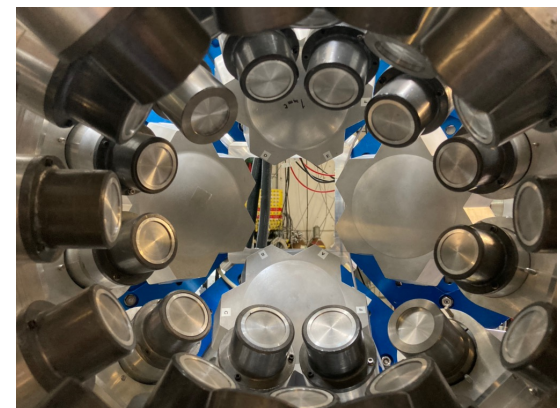


The γ detector array

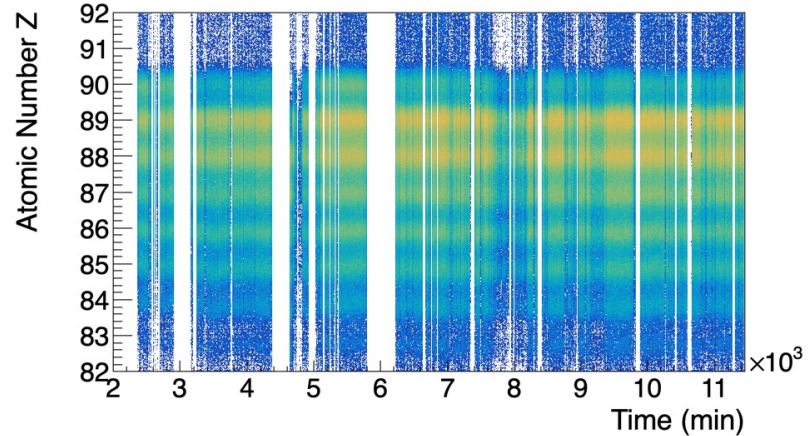
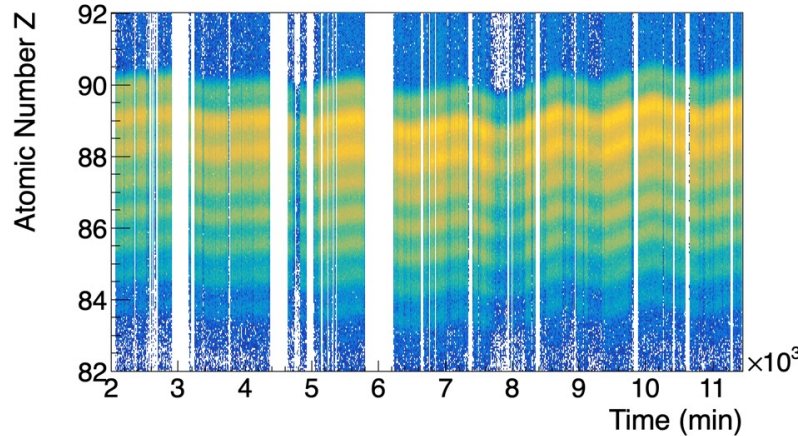
FATIMA - 36 LaBr₃(Ce) detectors



HPGe - 4 EUROBALL 7-fold clusters

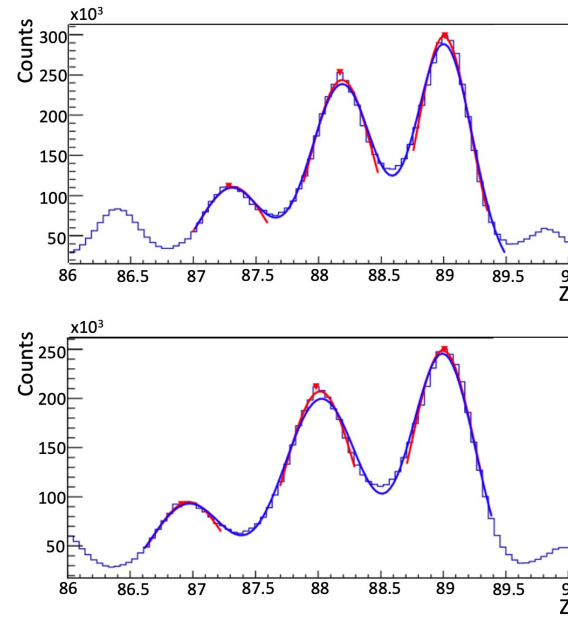


MUSIC: calibration and gain-matching

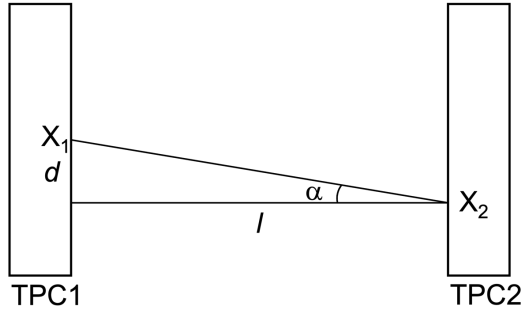


Two methods:

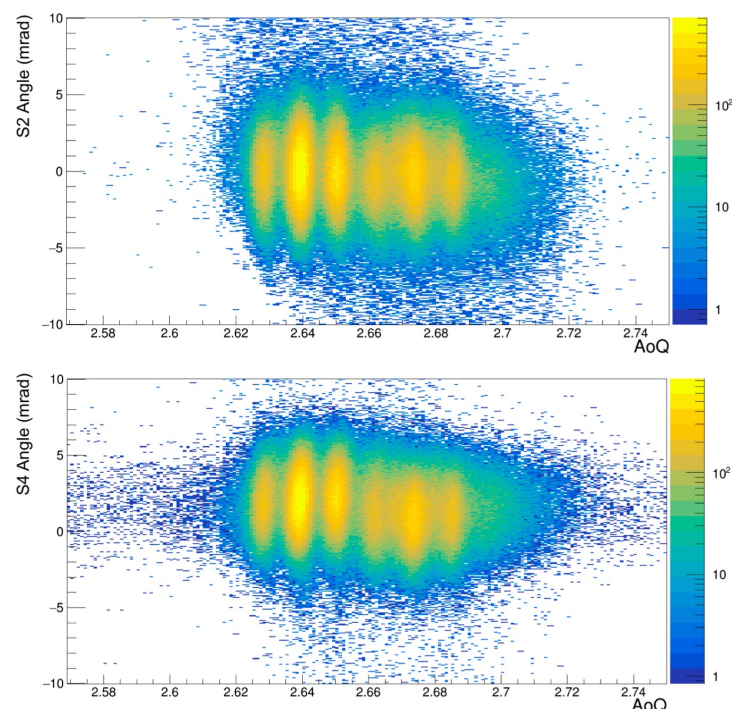
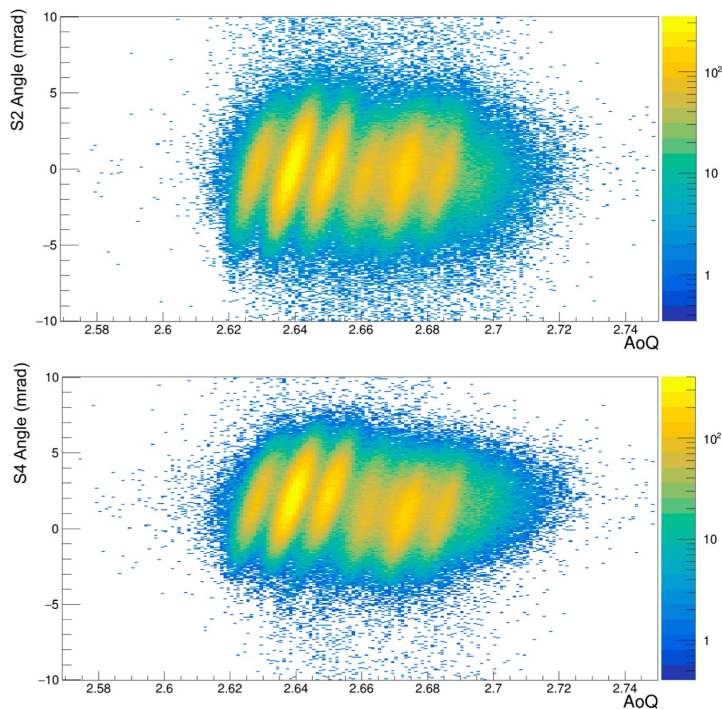
- Offset calculated between the strongest Z peak and the correspondent $Z=89$
- Linear calibration considering $Z=87,88,89$



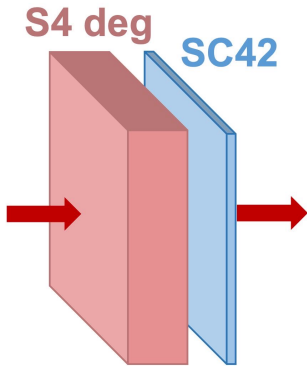
Angle correction



- The ions' trajectory is defined by their $B\rho$, which has a dependence on A/Q
- Aberrations of beam optics → angular dispersion of $\sim 10\text{mrad}$



S4 degrader thickness calibration

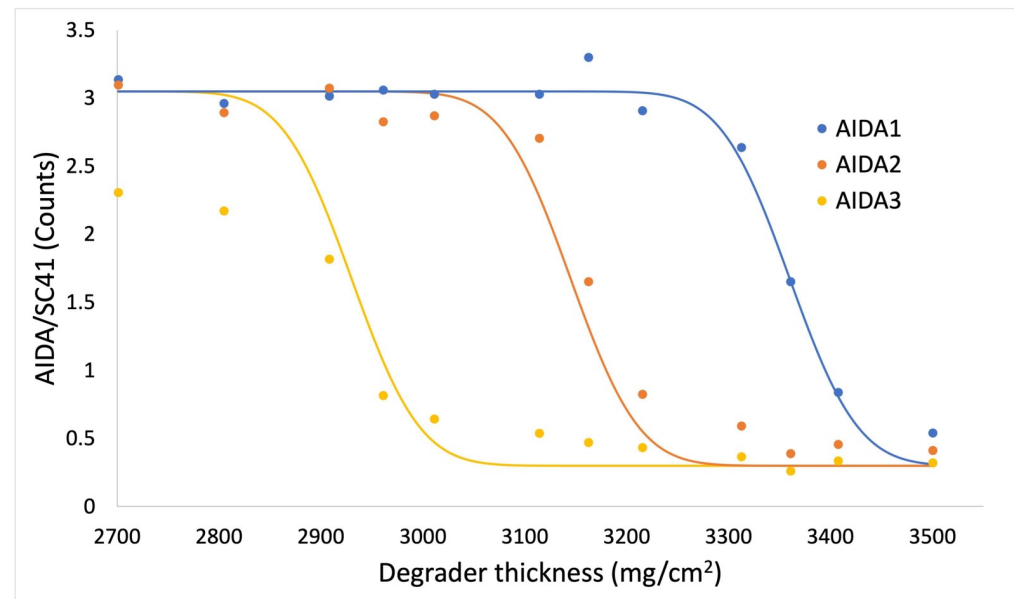


Procedure:

- low intensity primary beam and varying the degrader thickness
- rate ratio between AIDA layers and SC41

Calculated degrader offset:

~ 165 mg/cm².



Specific setup for S496

Triple AIDA and bPlast

- $24 \times 8 \text{ cm}^2$
- $384 \times 128 \text{ strips (49152 pixels)}$

